Five- and Six-Coordinate Group 4 Compounds Stabilized by β-Ketiminate and Diketiminate Ligands: Syntheses and Comparisons between Solid-State and Solution Structures

Lena Kakaliou, William J. Scanlon, IV, Baixin Qian, Sung W. Baek, and Milton R. Smith, III*,†

Department of Chemistry, Michigan State University, East Lansing, Michigan 48824

Douglas H. Motry

Department of Chemistry, Kent State University, Salem Campus, Salem, Ohio 44460-9412

Received November 25, 1998

The preparation and reaction chemistry of β-diketiminate titanium and zirconium complexes is described. Amine elimination reactions work well for introducing Tolnacnac or Tolnacac to the metal centers (TolnacnacH = 2-(*p*-tolylamino)-4-(*p*-tolylimino)-2-pentene; TolnacacH = 4-*p*-toluidinopent-3-en-2-one). In certain cases, the iminium salt of the diketimine can be used to circumvent the unfavorable reaction kinetics. Salt elimination reactions starting from group 4 metal halides and β-diketiminate lithium reagents are the most versatile method for introducing β-diketiminate ligands to the metal. For (β-diketiminate)MCl_3 compounds (M = Ti, Zr) η^5- and η^2-coordination modes can be controlled by modifying the diketiminate ligands. Several structures of five- and six-coordinate metal complexes were solved by X-ray diffraction methods. Five-coordinate metal complexes adopt both trigonal bipyramidal and square pyramidal geometries, and the six-coordinate metal complexes possess pseudooctahedral metal centers. For $(Tolnacnac)_2ZrX_2$ (X = Cl, OR, NMe_2) the activation parameters for Λ/Δ conversion have been probed by dynamic NMR and are consistent with a Bailar-twist mechanism. At a common temperature, the isomerization rates follow the order Cl > OR > NMe_2.

Introduction

Several groups have developed anionic nitrogen chelating ligands to complement cyclopentadienyl and porphyrin ligands.[1−10] In addition to fundamentally new discoveries in small-molecule activation chemistry, new classes of α-olefin polymerization catalysts that exhibit "living" behavior have been discovered.[11,12] In most cases, nitrogen ligands have been arranged in a dianionic motif as analogues to bis(cyclopentadienyl) systems.[10,12−15]

In addition to cyclopentadienyl ligands, amides and alkoxides are two of the most commonly used monodentate anionic ligands. The importance of ligand design is reflected by chemistry in tris(amido) C_{3v} ligand systems where the chemistry of polydentate tris(amide) ligands and amide ligands differ significantly.[5,16−18] Dianionic and trianionic ligand sets are well-suited for middle transition element chemistry; however, in early metal systems their use can restrict the number of redox sites that are available.

With the goal of studying compounds supported by monoanionic ligands whose steric and electronic properties can be easily modified, we have been examining the synthesis, structure, and reactivity of main-group and transition metal compounds stabilized by β-diketiminate ligands. This ligand family is a subset of Schiff base ligands[19] and has been known for many years with initial interest driven by their influence on the electronic structure of coordination compounds.[20,21] In their deprotonated form, these uninegative, four-electron donors can be viewed as hemiporphyrinate ligands with lower coordination numbers than cyclopentadienyl and tris(pyrazolyl)borate ligands. Diketiminate ligands share some similarities with amidinate ligands as both are monoanions in their deprotonated forms.[8,22]

† Fax: (517) 353-1793. Tel: (517) 355-9715 ext. 166, E-mail: smithmil@pilot.msu.edu.

(1) Lappert, M. F.; Liu, D.-S. *J. Organomet. Chem.* **1995**, *500*, 203−217.
(2) Killian, C. M.; Tempel, D. J.; Johnson, L. K.; Brookhart, M. *J. Am. Chem. Soc.* **1996**, *118*, 11664−11665.
(3) Dawson, D. Y.; Sangalang, J. C.; Arnold, J. *J. Am. Chem. Soc.* **1996**, *118*, 6082−6083.
(4) Cummins, C. C. *Prog. Inorg. Chem.* **1998**, *47*, 685−836.
(5) Schrock, R. R. *Acc. Chem. Res.* **1997**, *30*, 9−16.
(6) Black, D. G.; Jordan, R. F.; Rogers, R. D. *Inorg. Chem.* **1997**, *36*, 103−108.
(7) Fryzuk, M. D.; Love, J. B.; Rettig, S. J.; Young, V. G. *Science* **1997**, *275*, 1445−1447.
(8) Brussee, E. A. C.; Meetsma, A.; Hessen, B.; Teuben, J. H. *Organometallics* **1998**, *17*, 4090−4095.
(9) Scollard, J. D.; McConville, D. H.; Rettig, S. J. *Organometallics* **1997**, *16*, 1810−1812.
(10) Gibson, V. C.; Maddox, P. J.; Newton, C.; Redshaw, C.; Solan, G. A.; White, A. J. P.; Williams, D. J. *J. Chem. Soc., Chem. Commun.* **1998**, 1651−1652.
(11) Baumann, R.; Davis, W. M.; Schrock, R. R. *J. Am. Chem. Soc.* **1997**, *119*, 3830−3831.
(12) Scollard, J. D.; McConville, D. H. *J. Am. Chem. Soc.* **1996**, *118*, 10008−10009.
(13) Mountford, P. *Chem. Soc. Rev.* **1998**, *27*, 105−115.
(14) Cotton, F. A.; Czuchajowska, J. *Polyhedron* **1990**, *9*, 2553−2566.
(15) Warren, T. H.; Schrock, R. R.; Davis, W. M. *Organometallics* **1996**, *15*, 562−569.
(16) Budzichowski, T. A.; Chisholm, M. H.; Huffman, J. C.; Kramer, K. S.; Eisenstein, O. *J. Chem. Soc., Dalton Trans.* **1998**, 2563−2568.
(17) Cummins, C. C. *J. Chem. Soc., Chem. Commun.* **1998**, 1777−1786.
(18) Verkade, J. G. *Coord. Chem. Rev.* **1994**, *137*, 233−295.
(19) For seminal contributions by Bradley, Holm, Floriani, et al. to the development early transition metal Schiff base complexes, see: McAuliffe, C. A.; Barratt, D. S. *Comprehensive Coordination Chemistry*; McAuliffe, C. A., Barratt, D. S., Eds.; Pergamon Press: Oxford, U.K., 1987; Vol. 3, Chapters 31−33.
(20) Parks, J. E.; Holm, R. H. *Inorg. Chem.* **1968**, *7*, 1408−1416.
(21) McGeachin, S. G. *Can. J. Chem.* **1968**, *46*, 1903−1912.

10.1021/ic981364j CCC: $18.00
Published on Web 12/04/1999

In addition to having a larger bite angle, β-diketiminate ligands have six electrons in the π-manifold and can be viewed as heteroatom analogues of pentadienyl ligands.

Applications of β-diketiminate ligands to organometallic chemistry have been limited despite several attractive features.[23−31] First, they can be prepared in high yields from cheap and readily available building blocks, 2,4-pentanedione and primary amines.[32,33] Second, steric and electronic requirements can be modulated by varying the amine. Last, this ligand family can provide kinetic stability while maintaining several accessible oxidation states at the metal since they can ligate in neutral or uninegative forms. In this paper we outline the scope and limitations for preparing halide, amide, and alkoxide complexes of mono- and diketiminate group 4 complexes. We have also compared solid-state and solution structures and have measured activation parameters for stereoisomerism, recently described by Collins and co-workers for several zirconium bis(diketiminate) derivatives.[25]

Experimental Section

General Considerations. All manipulations were carried out using standard Schlenk techniques. Solvents were freshly distilled over sodium/benzophenone ketyl and were saturated with dinitrogen before use. Elemental analyses (C, H, N) were performed on a Perkin-Elmer CHN 2400 Series II CHNS/O analyzer at the Chemistry Department of MSU. A Varian VXR-300 NMR spectrometer was used to record ^{1}H (299.96 MHz) and ^{13}C (75.43 MHz) NMR spectra unless noted otherwise. ^{1}H and ^{13}C chemical shifts were referenced to the residual solvent peaks. Deuterated benzene was dried over activated 4-Å molecular sieves and vacuum transferred to a sodium-mirrored air-free flask. Uncorrected melting points of crystalline samples in sealed capillaries (under an argon atmosphere) were reported as ranges. Titanium tetrachloride was distilled and zirconium tetrachloride was sublimed before use. Tetrakis(dimethylamino)titanium,[34] tetrakis(dimethylamino)zirconium,[35] tetrabenzylzirconium,[36] zirconium tetrachloride bis(thf),[37] DipnacnacH,[38] TolnacnacH,[20] and Li(Tolnacnac)[26] were prepared according to the literature methods (Chart 1).

(Tolnacac)$_2$Zr(NMe$_2$)$_2$ (1). TolnacacH (370 mg, 1.90 mmol) in 20 mL of pentane was added dropwise to a stirred solution of Zr(NMe$_2$)$_4$ (260 mg, 0.97 mmol) in 2 mL of pentane at room temperature. Upon completion of the addition, a yellow solid precipitated. The solid was allowed to settle and the supernatant was decanted via cannula. The solid was pure as judged by ^{1}H NMR but could be recrystallized from pentane if necessary. The filtrate was reduced in volume and placed in a −80 °C freezer to yield another crop of yellow crystals (combined 355 mg, 66%): mp 164−166 °C; ^{1}H NMR (C_6D_6) δ 6.97 (s, 2 H, $C_6H_4CH_3$), 6.94 (s, 1 H, $C_6H_4CH_3$), 6.66 (s, 1 H, $C_6H_4CH_3$), 4.95 (s, 1 H, $CH_3C(O)CHC(NAr)CH_3$), 3.30 (s, 6 H, $N(CH_3)_2$), 2.16 (s, 3 H, $C_6H_4CH_3$), 1.56 (s, 3 H, CH_3), 1.42 (s, 3 H, CH_3); ^{13}C{^{1}H} NMR (C_6D_6) δ 173.90, 168.91, 148.26, 133.19, 129.15, 128.87, 124.46, 123.41, 102.78, 44.56, 24.41, 23.39, 20.83. Anal. Calcd for $C_{28}H_{40}N_4O_2Zr$: C, 60.50. H, 7.25; N, 10.08. Found: C, 60.02; H, 7.39; N, 9.90.

Chart 1[a]

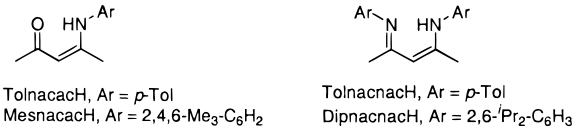

TolnacacH, Ar = *p*-Tol
MesnacacH, Ar = 2,4,6-Me$_3$-C$_6$H$_2$

TolnacnacH, Ar = *p*-Tol
DipnacnacH, Ar = 2,6-^{i}Pr$_2$-C$_6$H$_3$

[a] In previous papers, we abbreviated 2-(*N*-*p*-tolylamino)-4-(*N*-*p*-tolylimino)-2-pentene as TTPH and the corresponding diketiminate as TTP. In a recent report, Theopold has used the general abbreviation Rnacnac for diketiminates derived from primary amines, RNH_2.[30] Hereafter, we will use this nomenclature since it highlights the relationship to the acetylacetonate (acac) ligand and avoids confusion with the accepted designator for the tetratolylporphyrin ligand.

2-(Dimethylamino)-4-(*p*-tolylimino)-2-pentene (2). TolnacacH (1.1 g 5.87 mmol) in 3 mL of toluene was added via cannula to 29 mL of 0.1 M toluene solution of Ti(NMe$_2$)$_4$ (2.9 mmol) at room temperature. The reaction mixture turned a bright red color immediately. The reaction mixture was then heated to reflux for 24 h. The yellow solution was then filtered, and toluene was removed in a vacuum. The resulting orange solid was recrystallized from hexanes at −80 °C (570 mg, 89.5%): mp 35−36 °C; ^{1}H NMR (C_6D_6) δ 7.07 (d, J = 7.9 Hz, 2 H, $C_6H_4CH_3$), 6.89 (d, J = 7.9 Hz, 2 H, $C_6H_4CH_3$), 4.76 (s, 1 H, $CH_3C(NR)CHC(NR')CH_3$), 2.58 (s, 3 H, $C_6H_4CH_3$), 2.29 (s, 6 H, $N(CH_3)_2$), 2.19 (s, 3 H, $CH_3C(NR)CHC(NR')CH_3$), 1.92 (s, 3 H, $CH_3C(NR)CHC(NR')CH_3$); ^{13}C{^{1}H} NMR (C_6D_6) δ 164.34, 154.58, 151.79, 130.58, 129.66, 120.74, 98.05, 39.12, 22.99, 20.90, 16.77. Anal. Calcd for $C_{14}H_{20}N_2$: C, 77.73; H, 9.32; N, 12.94. Found: C, 77.39; H, 9.37; N, 12.75.

TiCl$_4$(TolnacacH)$_2$ (3). TolnacacH (800 mg, 4.23 mmol) in 4 mL of thf was added dropwise to a stirred solution of TiCl$_4$(thf)$_2$ (700 mg, 2.10 mmol) in 25 mL of thf at room temperature. After 2 h of stirring, the mixture was filtered leaving a dark red-purple solid behind. This solid was washed with pentane (2 × 7 mL) and dried under vacuum. A second crop was isolated from the filtrate at −80 °C (combined, 570 mg, 90%): mp 155 °C (dec); ^{1}H NMR ($CDCl_3$) δ 12.62 (s, 1 H, N*H*), 7.20 (d, J = 8.8 Hz, 2 H, $C_6H_4CH_3$), 7.13 (d, J = 8.8 Hz, 2 H, $C_6H_4CH_3$), 5.35 (s, 1 H, $CH_3C(O)CHC(NHAr)CH_3$), 2.69 (s, 3 H, $C_6H_4CH_3$), 2.33 (s, 3 H, CH_3), 2.13 (s, 3 H, CH_3). Anal. Calcd for $C_{24}H_{30}N_2Cl_4O_2Ti$: C, 50.73; H, 5.32; N, 4.93. Found: C, 49.08; H, 5.10; N, 4.42.

TiCl$_4$(MesnacacH)$_2$ (4). TiCl$_4$(MesnacacH)$_2$ was synthesized analogously to **3** from (Mesnacac)H and TiCl$_4$(thf)$_2$ in 89% yield as a maroon solid: mp 130 °C (dec), ^{1}H NMR ($CDCl_3$) δ 12.12 (s, 1 H, N*H*), 6.85 (s, 2 H, $C_6H_2(CH_3)_2CH_3$), 5.33 (s, 1 H, $CH_3C(O)CHC(NHAr)CH_3$), 2.65 (s, 3 H, $C_6H_2(CH_3)_2CH_3$), 2.24 (s, 3 H, CH_3), 2.19 (s, 6 H, $C_6H_2(CH_3)_2CH_3$) 1.84 (s, 3 H, CH_3); ^{13}C{^{1}H} NMR (C_6D_6) δ 191.24, 172.18, 138.72, 134.50, 132.26, 129.28, 97.83, 26.00, 20.98, 20.44, 18.36. Anal. Calcd for $C_{30}H_{42}N_2Cl_4O_{2.5}Ti$ or **3b**(thf)$_{0.5}$: C, 54.56; H, 6.41; N, 4.24. Found: C, 54.77; H, 6.68; N, 4.12.

(Tolnacnac)Ti(NMe$_2$)$_3$ (5). TolnacnacH (3.8 g, 13.8 mmol) in 5 mL of toluene was added dropwise to a stirred solution of Ti(NMe$_2$)$_4$ (3.36, g 13.8 mmol) at room temperature. The reaction mixture was heated at 35 °C overnight. The toluene was removed under vacuum. Orange crystals were recrystallized from pentane at −80 °C. (5.5 g, 87%): mp 140−143 °C; ^{1}H NMR (C_6D_6) δ 6.95 (d, J = 9.0 Hz, 4 H, $C_6H_4CH_3$), 6.65 (d, J = 9.0 Hz, 4 H, $C_6H_4CH_3$), 5.21 (s, 1 H, $CH_3C(NAr)CHC(NAr)CH_3$), 2.95 (s, 18 H, $N(CH_3)_2$), 2.13 (s, 6 H, $C_6H_4CH_3$), 1.78 (s,

(22) Hagadorn, J. R.; Arnold, J. *Angew. Chem., Int. Ed. Engl.* **1998**, *37*, 1729−1731.
(23) Hitchcock, P. B.; Hu, J.; Lappert, M. F.; Layh, M.; Liu, D. S.; Severn, J. R.; Tian, S. *An. Quim.* **1996**, *92*, 266−266.
(24) Feldman, J.; McLain, S. J.; Parthasarathy, A.; Marshall, W. J.; Calabrese, J. C.; Arthur, S. D. *Organometallics* **1997**, *16*, 1514−1516.
(25) Rahim, M.; Taylor, N. J.; Xin, S.; Collins, S. *Organometallics* **1998**, *17*, 1315−1323.
(26) Qian, B.; Ward, D. L.; Smith, M. R., III. *Organometallics* **1998**, *17*, 3070−3076.
(27) Cheng, M.; Lobkovsky, E. B.; Coates, G. W. *J. Am. Chem. Soc.* **1998**, *120*, 11018−11019.
(28) Budzelaar, P. H. M.; de Gelder, R.; Gal, A. W. *Organometallics* **1998**, *19*, 4121−4123.
(29) Radzewich, C. E.; Coles, M. P.; Jordan, R. F. *J. Am. Chem. Soc.* **1998**, *120*, 9384−9385.
(30) Kim, W.-K.; Fevola, M. J.; Liable-Sands, L. M.; Rheingold, A. L.; Theopold, K. H. *Organometallics* **1998**, *17*, 4541−4543.
(31) Qian, B.; Scanlon, W. J., IV; Smith, M. R., III; Motry, D. H. *Organometallics* **1999**, *18*, 1693−1698.
(32) Scheibe, G. *Chem. Ber.* **1923**, *56*, 137−148.
(33) A clever alternative route to β-diketiminates from isonitriles and alkyllithium reagents has recently been described: Hitchcock, P. B.; Lappert, M. F.; Layh, M. *J. Chem. Soc., Chem. Commun.* **1998**, 201−202.
(34) Naiini, A. A.; Ringrose, S. L.; Su, Y.; Jacobson, R. A.; Verkade, J. G. *Inorg. Chem.* **1993**, *32*, 1290−1296.
(35) Bradley, D. C.; Thomas, I. M. *J. Chem. Soc.* **1960**, 3857−3861.
(36) Zucchini, U.; Albizzati, E.; Giannini, U. *J. Organomet. Chem.* **1971**, *26*, 357−372.
(37) Manzer, L. E. *Inorg. Synth.* **1982**, *21*, 135−136.
(38) Clegg, W.; Cope, E. K.; Edwards, A. J.; Mair, F. S. *Inorg. Chem.* **1998**, *37*, 2317−2319.

6 H, C*H*$_3$C(NAr)CHC(NAr)C*H*$_3$); ^{13}C{^{1}H} NMR (C_6D_6) δ 162.81, 150.16, 132.28, 128.57, 124.70, 100.24, 46.23, 24.43, 20.84. Anal. Calcd for $C_{25}H_{39}N_5Ti$: C, 65.63; H, 8.59; N, 15.31. Found: C, 65.70; H, 8.75, N, 15.01.

(Tolnacnac)Zr(NMe$_2$)$_3$ (6). TolnacnacH (1.30 g, 0.467 mmol) in 2 mL of toluene was added dropwise to a stirred solution of Zr(NMe$_2$)$_4$ (1.25 g, 0.467 mmol) in 2 mL of toluene at room temperature. After stirring of the solution for 1 h, toluene was removed under vacuum leaving an orange-yellow solid (2.26 g, 98%): mp 117−119 °C; ^{1}H NMR (C_6D_6) δ 6.98 (d, J = 8 Hz, 4 H, C$_6$*H*$_4$CH$_3$), 6.76 (d, J = 8 Hz, 4 H, C$_6$*H*$_4$CH$_3$), 5.10 (s, 1 H, CH$_3$C(NAr)C*H*C(NAr)CH$_3$), 2.80 (s, 18 H, N(C*H*$_3$)$_2$), 2.12 (s, 6 H, C$_6$H$_4$C*H*$_3$), 1.75(s, 6 H, C*H*$_3$C(NAr)CHC(NAr)C*H*$_3$); ^{13}C{^{1}H} NMR (C_6H_6) δ 164.54, 148.26, 133.04, 129.15, 125.08, 100.23, 42.41, 24.21, 20.84. Anal. Calcd for $C_{25}H_{39}N_5Zr$: C, 59.95; H, 7.85; N, 13.98. Found: C, 59.59; H, 7.48; N, 13.89.

(Tolnacnac)$_2$Zr(NMe$_2$)$_2$ (7). TolnacnacH (2.1 g, 7.5 mmol) in 5 mL of toluene was added dropwise to a solution of Zr(NMe$_2$)$_4$ (1.01 g, 3.8 mmol) in 5 mL of toluene. After the solution was allowed to stir at 90 °C for 5 h, toluene was removed under vacuum and the resulting solid was recrystallized from pentane yielding orange-yellow crystals (1.6 g, 58%): mp 190−195 °C; ^{1}H NMR (C_6D_6) δ 7.25 (m, 4 H, C$_6$*H*$_4$CH$_3$), 7.07 (m, 4 H, C$_6$*H*$_4$CH$_3$), 6.87 (m, 6 H, C$_6$*H*$_4$CH$_3$), 5.67 (m, 2 H, C$_6$*H*$_4$CH$_3$), 5.13 (s, 2 H, CH$_3$C(NAr)C*H*C(NAr)CH$_3$), 2.64 (broad s, 12 H, N(C*H*$_3$)$_2$), 2.22 (s, 6 H, C$_6$H$_4$C*H*$_3$), 2.06 (s, 6 H, C$_6$H$_4$C*H*$_3$), 1.77 (s, 6 H, C*H*$_3$C(NAr)CHC(NAr)CH$_3$), 1.43 (s, 6 H, CH$_3$C(NAr)CHC(NAr)C*H*$_3$); ^{13}C{^{1}H} NMR (C_6H_6) δ 164.90, 164.33, 150.35, 149.99, 133.78, 133.07, 128.93, 128.47, 128.42, 127.20, 125.78, 100.50, 46.45, 25.81, 25.58, 20.96, 20.85. Anal. Calcd for $C_{42}H_{54}N_6Zr$: C, 68.74. H, 7.36; N, 11.44. Found: C, 68.97; H, 7.35; N, 10.70.

(Dipnacnac)ZrCl(NMe$_2$)$_2$ (8). Zr(NMe$_2$)$_4$ (250 mg, 0.93 mmol) in 2 mL of toluene was added dropwise to a stirred suspension of DipnacnacH·HCl (430 mg, 0.94 mmol) in 2 mL of toluene at −78 °C. Once the addition was complete, the mixture was allowed to warm to room temperature. All solids dissolved leaving a clear green solution. The reaction mixture was allowed to stir overnight. After toluene was removed under vacuum, the remaining solid was recrystallized from pentane yielding small colorless crystals (300 mg, 51%): mp 197−199 °C; ^{1}H NMR (C_6D_6) at 50 °C δ 7.12 (m, 6 H, C$_6$*H*$_3$(CH(CH$_3$)$_2$)$_2$), 5.20 (s, 1 H, CH$_3$C(NAr)C*H*C(NAr)CH$_3$), 3.03 (sept, J = 6.9 Hz, 4 H, C$_6$H$_3$(C*H*(CH$_3$)$_2$)$_2$), 2.70 (s, 12 H, N(C*H*$_3$)$_2$), 1.63 (s, 6 H, C*H*$_3$C(NAr)CHC(NAr)C*H*$_3$), 1.37 (d, J = 6.8 Hz, 12 H, C$_6$H$_3$(CH(C*H*$_3$)$_2$)$_2$), 1.15 (d, J = 6.8, 12 H, C$_6$H$_3$(CH(C*H*$_3$)$_2$)$_2$); ^{13}C{^{1}H} NMR (C_6D_6) at 50 °C δ 167.02, 149.29, 141.69, 126.05, 123.90, 100.84, 41.73, 29.104, 25.95, 25.13, 24.27. Anal. Calcd for $C_{33}H_{53}N_4ClZr$: C, 62.58; H, 8.45; N, 8.85. Found: C, 62.50; H, 8.61; N, 8.62.

(Tolnacac)$_2$TiCl$_2$ (9). Li(Tolnacac) (580 mg, 2.99 mmol) in 5 mL of methylene chloride was added dropwise to a solution of TiCl$_4$(thf)$_2$ (500 mg, 1.49 mmol) in 20 mL of methylene chloride at room temperature. After 2 h of stirring, the mixture was filtered and precipitates were extracted with pentane. The volume of the combined filtrate was reduced under vacuum. Layering the solution with pentane and placing it in a −80 °C freezer resulted in red crystals (590 mg, 80%): mp 163−165 °C (dec); ^{1}H NMR ($CDCl_3$) δ 7.17 (m, 2 H, C$_6$*H*$_4$CH$_3$), 7.02 (d, J = 7.5 Hz, 1 H, C$_6$*H*$_4$CH$_3$), 6.48 (d, J = 8.1 Hz, 1 H, C$_6$*H*$_4$CH$_3$), 5.31 (s, 1 H, CH$_3$C(OH)C*H*C(NAr)CH$_3$), 2.31 (s, 3 H, C$_6$H$_4$C*H*$_3$), 1.66 (s, 3 H, C*H*$_3$), 1.33 (s, 3 H, C*H*$_3$); ^{13}C{^{1}H} NMR ($CDCl_3$) δ 175.42, 169.76, 148.79, 135.07, 129.40, 128.55, 125.70, 121.78, 109.51, 24.41,22.04, 20.82. Anal. Calcd for $C_{24}H_{28}N_2Cl_2O_2Ti$: C, 58.20; H, 5.70; N, 5.65. Found: C, 58.13; H, 5.98; N, 5.52.

(Tolnacac)$_2$ZrCl$_2$ (10). (Tolnacac)$_2$ZrCl$_2$ was synthesized analogously to **9** as pale yellow crystals from Li(Tolnacac) and ZrCl$_4$(thf)$_2$ in 78.5% yield: mp 205−207 °C (dec); ^{1}H NMR ($CDCl_3$) δ 7.12 (m, 3 H, C$_6$*H*$_4$CH$_3$), 6.51 (m 1 H, C$_6$*H*$_4$CH$_3$), 5.22 (s, 1 H, CH$_3$C(O)C*H*C(NAr)CH$_3$), 2.32 (s, 3 H, C$_6$H$_4$C*H*$_3$), 1.69 (s, 3 H, C*H*$_3$), 1.33 (s, 3 H, C*H*$_3$); ^{13}C{^{1}H} NMR ($CDCl_3$) δ 174.85, 173.09, 145.82, 135.16, 129.92, 129.40, 125.49, 122.84, 106.28, 24.52, 22.78, 20.84. Anal. Calcd for $C_{24}H_{28}N_2Cl_2O_2Zr$: C, 53.52; H, 5.24; N, 5.20. Found: C, 53.58; H, 5.33; N, 5.11.

(Mesnacac)$_2$TiCl$_2$ (11). (Mesnacac)$_2$TiCl$_2$ was synthesized analogously to **9** from Li(Mesnacac) and TiCl$_4$(thf)$_2$ in 70.3%: mp 125−126 °C (dec); ^{1}H NMR ($CDCl_3$) δ 6.86 (s, 1 H, C$_6$*H*$_2$(CH$_3$)$_2$CH$_3$), 6.77 (s, 1 H, C$_6$*H*$_2$(CH$_3$)$_2$CH$_3$), 5.80 (s, 1 H, CH$_3$C(O)C*H*C(NAr)CH$_3$), 2.27 (s, 3 H, C*H*$_{3\ \text{mesityl}}$), 2.24 (s, 3 H, C*H*$_{3\ \text{mesityl}}$), 2.06 (s, 3 H, C*H*$_{3\ \text{mesityl}}$), 1.85 (s, 3 H, C*H*$_3$), 1.69 (s, 3 H, C*H*$_3$); ^{13}C{^{1}H} NMR ($CDCl_3$) δ 176.57, 172.16, 146.51, 135.42, 132.40, 129.77, 128.98, 128.15, 109.65, 23.44, 22.61, 20.94, 19.73, 18.67.

(Mesnacac)$_2$ZrCl$_2$ (12). (Mesnacac)$_2$ZrCl$_2$ was synthesized analogously to **9** as a white powder from Li(Mesnacac) and ZrCl$_4$(thf)$_2$ in 78.5%: mp 195−198 °C (dec); ^{1}H NMR ($CDCl_3$) δ 6.85 (br s, 2 H, C$_6$*H*$_2$(CH$_3$)$_2$CH$_3$), 5.58 (s, 1 H, CH$_3$C(O)C*H*C(NAr)CH$_3$), 2.24 (s, 3 H, C$_6$H$_3$(CH$_3$)$_2$C*H*$_3$), 2.19 (s, 6 H, C$_6$H$_3$(C*H*$_3$)$_2$CH$_3$), 1.93 (s, 3 H, C*H*$_3$), 1.68 (s, 3 H, C*H*$_3$); ^{13}C{^{1}H} NMR ($CDCl_3$) δ 175.41, 174.88, 143.59, 135.50, 134.30, 129.34, 106.39, 23.55, 20.90, 18.89, 18.10.

(Tolnacnac)TiCl$_3$ (13). Li(Tolnacnac) (1.43 g 5.03 mmol) in 10 mL of toluene was added to a toluene solution of TiCl$_4$ (2.6 mL of 1.8 M, 4.7 mmol) at room temperature. The mixture turned dark immediately upon addition and was slightly exothermic. The reaction mixture was stirred for 2 h. The dark solution was removed via cannula, and the remaining dark solid was extracted with hot toluene. The filtrates were combined, and their volume was reduced under vacuum. Dark purple plates were grown at −80 °C (1.6 g, 84%): mp 125−127 °C; ^{1}H NMR ($CDCl_3$) δ 7.23−7.13 (m, 8 H, C$_6$*H*$_4$CH$_3$), 6.03 (s, 1 H, CH$_3$C(NAr)C*H*C(NAr)CH$_3$), 2.36 (s, 6 H, C$_6$H$_4$C*H*$_3$), 2.12 (s, 6 H, C*H*$_3$C(NAr)CHC(NAr)C*H*$_3$); ^{13}C{^{1}H} NMR ($CDCl_3$) δ 159.82, 146.62, 129.73, 123.82, 104.86, 22.72, 21.12. Anal. Calcd for $C_{26}H_{29}N_2Cl_3Ti$: C, 59.62. H, 5.58; N, 5.35. Found: C, 59.29; H, 5.33, N, 5.22.

(Dipnacnac)ZrCl$_3$(thf) (14). Li(Dipnacnac) (450 mg, 1.15 mmol) in 2 mL of toluene was added dropwise to a stirred suspension of ZrCl$_4$(thf)$_2$ (430 mg, 1.14 mmol) in 2 mL of toluene at room temperature. After the addition was completed, the solution was allowed to stir overnight. The clear orange solution was filtered off via cannula. The filtrate was reduced in volume under vacuum and then cooled to −80 °C yielding small yellow crystals (390 mg 49%): mp > 225 °C; ^{1}H NMR (C_6D_6) δ 7.15 (m, 6 H, C$_6$*H*$_3$(CH(CH$_3$)$_2$)), 5.43 (s, 1 H, CH$_3$C(NAr)C*H*C(NAr)CH$_3$), 3.90 (m, 4 H, *thf*), 3.58 (septet, J = 6.8 Hz, 4H, C$_6$H$_3$C*H*(CH$_3$)$_2$)), 1.65 (s, 6H, C*H*$_3$C(NAr)CHC(NAr)C*H*$_3$), 1.54 (d, J = 6.8 Hz, 6 H, C$_6$H$_3$CH(C*H*$_3$)$_2$), 1.10 (d, J = 6.8, 6H, C$_6$H$_3$CH(C*H*$_3$)$_2$), 1.05 (m, 4H, *thf*); ^{13}C{^{1}H} NMR (C_6H_6) δ 169.33, 145.86, 144.08, 124.76, 105.64, 77.00, 28.93, 26.45, 25.66, 24.82, 24.74.

(Tolnacnac)ZrCl$_3$ (15). Freshly distilled chlorotrimethylsilane (1.3 g, 11 mmol) was mixed with (Tolnacnac)Zr(NMe$_2$)$_3$ (1.8 g, 3.6 mmol) in 20 mL of toluene. After being stirred at 60 °C for 24 h, the mixture was cooled to −30 °C overnight. The resultant precipitate was collected by filtration and washed with copious amount of pentane (0.68 g, 40%) to yield a yellow crystalline solid: mp > 220 °C; ^{1}H NMR ($CDCl_3$) δ 7.22 (m 8 H), 5.95 (s, 1 H), 2.38 (s, 6 H), 1.93 (s, 6 H); ^{13}C{^{1}H} NMR ($CDCl_3$) δ 167.0, 143.2, 136.9, 129.6, 127.3, 109.2, 24.10, 21.15. Anal. Calcd for $C_{19}H_{21}N_2Cl_3Zr$: C, 47.96; H, 4.45; N, 5.88. Found: C, 48.18; H, 4.57; N, 5.55.

(Tolnacnac)$_2$ZrCl$_2$ (16). A 5 mL toluene solution of Li(Tolnacnac) (1.55 g, 5.45 mmol) was cooled −78 °C and added dropwise to a stirred suspension of ZrCl$_4$(thf)$_2$ (1.11 g, 2.72 mmol) in 5 mL of toluene which was also at −78 °C. The reaction mixture was allowed to warm to room temperature. After 2 h of stirring, the mixture was filtered via cannula and the solid was extracted several times with hot toluene. The filtrates were combined. The volume was reduced under vacuum, and a yellow solid recrystallized from toluene/pentane (0.98 g, 50%): mp > 250 °C; ^{1}H NMR ($CDCl_3$) δ 7.01 (d, J = 8.1 Hz, 4 H, C$_6$*H*$_4$CH$_3$), 6.71 (m, 4 H, C$_6$*H*$_4$CH$_3$), 5.34 (s, 1 H, CH$_3$C(NAr)C*H*C(NAr)CH$_3$), 2.28 (s, 6 H, C$_6$H$_4$C*H*$_3$), 1.63 (s, 6 H, C*H*$_3$C(NAr)CHC(NAr)C*H*$_3$); ^{13}C{^{1}H} NMR ($CDCl_3$) δ 166.29, 146.03, 135.11, 128.61, 127.73, 105.32, 25.12, 20.96. Anal. Calcd for $C_{38}H_{42}N_4Cl_2Zr$: C, 63.66; H, 5.90; N, 7.81. Found: C, 63.70; H, 6.67; N, 7.78.

(Dipnacnac)ZrCl$_3$ (17). Li(Dipnacnac) (830 mg, 2.2 mmol) in 2 mL of toluene was added dropwise to a stirred suspension of ZrCl$_4$ (freshly sublimed) (500 mg, 2.1 mmol) in 2 mL of toluene. Several toluene washings (3 × 1 mL) were used to ensure complete Li(Dipnacnac) transfer. Once the addition was complete, the solution was allowed to stir overnight at 60 °C. The solution was filtered off via cannula while still warm. The solvent was removed under vacuum. The remaining orange solid was recrystallized from CH_2Cl_2 at −80 °C yielding small yellow crystals (670 mg, 50.7%): mp > 220 °C; ^{1}H

NMR ($CDCl_3$) δ 7.34−7.20 (m, 6 H, $C_6H_3CH(CH_3)_2$), 5.90 (s, 1 H, $CH_3C(NAr)CHC(NAr)CH_3$), 3.05 (septet, J = 6.9 Hz, 4 H, $C_6H_3CH(CH_3)_2$), 1.94 (s, 6 H, $CH_3C(NAr)CHC(NAr)CH_3$), 1.37 (d, J = 6.9 Hz, 6 H, $C_6H_3CH(CH_3)_2$), 1.18 (d, J = 6.9 Hz, 6H, $C_6H_3(CH(CH_3)_2)$; $^{13}C\{^1H\}$ NMR ($CDCl_3$) δ 171.3, 146.6, 141.7, 127.8, 124.6, 104.9, 29.1, 26.2, 24.7, 24.6. Anal. Calcd for $C_{29}H_{41}N_2Cl_3Zr$: C, 56.53; H, 6.71; N, 4.54. Found: C, 56.54; H, 6.59; N, 4.42.

(Tolnacnac)Zr(OMe)$_3$ (18). (Tolnacnac)Zr(NMe_2)$_3$ (0.50 g, 0.80 mmol) in 10 mL of toluene solution was treated with dry methyl alcohol in toluene solution (7.7 mL, 0.31 M, 2.4 mmol) at 0 °C with stirring. After the mixture was stirred at room temperature for 12 h, all volatile materials were removed under vacuum. A waxy solid formed and was washed with pentane. The residue was taken into toluene and recrystallized from toluene/pentane at −80 °C overnight as pale yellow solids (34 mg, 9%): mp 40−42 °C; ^1H NMR ($CDCl_3$) δ 7.08 (m, 4 H), 7.02 (m, 4 H), 4.99 (s, 1 H), 3.29 (br, s, 8 H), 2.30 (s, 6 H), 1.71 (s, 6 H); $^{13}C\{^1H\}$ NMR ($CDCl_3$) δ 164.22, 148.51, 132.93, 129.32, 126.50, 100.22, 56.71, 24.21, 20.81. Anal. Calcd for $C_{22}H_{30}N_2O_3Zr$: C, 57.18; H, 6.50; N, 6.06. Found: C, 56.83; H, 6.60; N, 6.17.

(Tolnacnac)$_2$Zr(OMe)$_2$ (19). (Tolnacnac)$_2$Zr(OMe)$_2$ was prepared in a fashion similar to the synthesis of **18** from (Tolnacnac)$_2$Zr(NMe_2)$_2$ and 2 equiv of MeOH in toluene as colorless solid in 45% yield after 12 h of stirring at room temperature: mp 45−48 °C; ^1H NMR (C_6D_6) δ 7.18 (m, 6 H), 7.14 (m, 4 H), 6.94 (d, J = 7.8 Hz, 4 H), 5.60 (m, 2 H), 5.01 (s, 2 H), 3.28 (s, 9 H), 2.32 (s, 6 H), 2.09 (s, 6 H), 1.80 (s, 6 H), 1.58 (s, 6 H); $^{13}C\{^1H\}$ NMR (C_6D_6) δ 165.1, 163.8, 149.4, 148.8, 133.4, 132.8, 129.7, 128.8, 127.4, 127.1, 101.0, 56.56, 24.51, 24,48, 21.00, 20.88. Anal. Calcd for $C_{40}H_{48}N_4O_2Zr$: C, 67.76; H, 6.82; N, 7.90. Found: C, 67.80; H, 7.18; N, 7.87.

(Tolnacnac)$_2$Zr(O-*p*-Tol)$_2$ (20). (Tolnacnac)$_2$Zr(NMe_2)$_2$ (0.49 g, 0.67 mmol) in 15 mL of pentane solution was treated with a suspension of 4-methylphenol (0.15 g, 1.3 mmol) in 20 mL of pentane at 0 °C with stirring. A yellow precipitate formed immediately upon addition and was collected by filtration and washed with pentane. The yellow product was further purified by recrystallization from toluene/pentane at −30 °C overnight (0.38 g, 67%): mp 239−242 °C (dec); ^1H NMR ($CDCl_3$) δ 7.05 (m, 10 H), 6.62 (m, 10 H), 5.77 (d, J = 8.1 Hz, 4 H), 4.97 (s, 2 H), 2.30 (s, br, 6 H), 2.16 (s, 6 H), 1.72 (s, br, 6 H), 1.36 (s, br, 6 H); $^{13}C\{^1H\}$ NMR ($CDCl_3$) δ 165.1, 164.9, 159.8, 147.1, 146.9, 134.0, 133.9, 128.6, 128.2, 128.1, 126.9, 126.7, 119.7, 101.2, 101.0, 24.63, 21.01, 20.68, 20.58, 20.42. Anal. Calcd for $C_{52}H_{56}N_4O_2Zr$: C, 72.54; H, 6.56; N, 6.50. Found: C, 72.37; H, 6.86; N, 6.52.

(Tolnacnac)$_2$Zr(OCH$_2$C$_6$H$_4$-4-*t*-Bu)$_2$ (21). (Tolnacnac)$_2$Zr(NMe_2)$_2$ (0.18 g, 0.24 mmol) in 10 mL of toluene was treated with a toluene solution of freshly distilled 4-*tert*-butylbenzyl alcohol (80 mg, 4.9 mmol) at −78 °C with stirring. The mixture was allowed to warm to room temperature and further stirred at that temperature for 5 min. After all volatile materials were removed under vacuum, the product was taken into pentane and crystallized at −80 °C after 2 days as a colorless solid (0.22 g, 92%): mp 70−75 °C; ^1H NMR (C_6D_6) δ 7.26 (m 12 H), 7.08 (m 4 H), 6.80 (m, 6 H), 5.58 (m, 2 H), 5.02 (s, 2 H), 4.32 (s, 4 H), 2.28 (s, 6 H), 2.08 (s, 6 H), 1.80 (s, 6 H), 1.55 (s, 6 H), 1.28 (s, 18 H); $^{13}C\{^1H\}$ NMR (C_6D_6) δ 165.2, 164.2, 149.2, 149.0, 148.8, 141.2, 133.6, 132.8, 128.9, 128.6, 127.8, 127.7, 126.8, 124.8, 100.8, 71.41, 34.44, 34.66, 24.89, 24.79, 21.00, 20.86. Anal. Calcd for $C_{60}H_{72}N_4O_2Zr$: C, 74.03; H, 7.46; N, 5.76. Found: C, 73.87; H, 7.80; N, 5.68.

Variable-Temperature NMR Spectroscopy. Variable-temperature ^1H NMR experiments were carried out on an Inova 300 MHz instrument. The temperature gauge was calibrated using methyl alcohol. Part of the ^1H NMR spectrum was converted into digital form, and the formatted y values were fed into the DNMR5 program.[39] The exchange rate was calculated. Activation parameters were obtained from the Eyring plots, i.e., ln(k/T) vs 1000/T, and results are listed in Table 10.

X-ray Structure Determination. X-ray-quality crystals of **1** were grown from hexane solution at −30 °C. The crystals were collected by filtration and coated with Paratone-*N*. A suitable single crystal was picked and mounted onto a glass fiber. The crystal was then transferred to the goniometer of a Siemens SMART CCD diffractometer using Mo Kα radiation (λ = 0.710 73 Å). Data were collected as 30 s per frame at 173 K. The initial cells were calculated by the Smart from three sets of 15 frames. All data sets were collected over a hemisphere of reciprocal space. SAINT was used to integrate 1025 frames and to generate the *raw* file. Final unit cell parameters were obtained by least-squares refinement of the strong reflections obtained. Absorption correction and time decay were applied to the data by SADABS. Atomic coordinates and thermal parameters were refined using the full-matrix least-squares program, SHELXL-97, and calculations were based on F^2 data. All non-hydrogen atoms were refined using anisotropic thermal parameters. All hydrogen atoms are put in ideal positions (HADD in XP) and refined as riding models. The choice of space group of $P2_1/c$ is based on systematic absence and the successful refinement of the structure. This structure was solved by the Patterson methods. Details are given in Table 1 and in the Supporting Information.

X-ray-quality crystals of **4** were grown from thf solutions at −30 °C. A procedure similar to that of **1** was followed. The choice of space group of $C2/c$ is based on systematic absence and the successful refinement of the structure. In the refined structure, two titanium atoms are on the special positions; i.e., Ti(1) is on a 2-fold axis while Ti(2) is on an inversion center. Details are given in Table 1 and in the Supporting Information.

X-ray-quality crystals of **5** were grown from hexane solution at −30 °C. A procedure similar to that of **1** was followed. The choice of space group of $P\bar{1}$ is based on the successful refinement of the structure. Details are given in Table 1 and in the Supporting Information.

X-ray-quality crystals of **6** were grown from hexane solution at −30 °C. A procedure similar to that of **1** was followed. The structure was partially solved in $P\bar{1}$. An inversion center between the two "independent molecules" was found. Its location was determined by calculating the difference of the absolute values of the x, y, and z coordinates for symmetrically related atoms. One of the two molecules was then discarded and the origin redetermined. The space group was changed to $P\bar{1}$. Details are given in Table 1 and in the Supporting Information.

X-ray-quality crystals of **8** were grown from hexane solution at −30 °C. A procedure similar to that of **1** was followed. The choice of space group of $P\bar{1}$ is based on the successful refinement of the structure. The final cell contained two crystallographically different but chemical identical molecules. Details are given in Table 1 and in the Supporting Information.

X-ray-quality crystals of **9** were grown from toluene/pentane solution at −30 °C. A procedure similar to that of **1** was followed. The choice of space group *Pbca* is based on systematic absence and intensity statistics. The structure was solved by the direct methods. Details are given in Table 1 and in the Supporting Information.

X-ray-quality crystals of **10** were grown from toluene/pentane solution at −30 °C. A procedure similar to that of **1** was followed. The choice of a noncentrosymmetric space group $P3_121$ is based on systematic absence and intensity statistics. This structure was solved by the Patterson methods. We were able to refine the absolute structure parameter to 0.01(3). Details are given in Table 1 and in the Supporting Information.

X-ray-quality crystals of **11** were grown from methylene chloride solution at −30 °C. A procedure similar to that of **1** was followed. The choice of space group $P\bar{1}$ is based on intensity statistics and the successful refinement of the structure. The structure was solved by the direct methods. Details are given in Table 1 and in the Supporting Information.

X-ray-quality crystals of **13** were grown from toluene solution at −30 °C. A procedure similar to that of **1** was followed. The structure was solved by the direct methods. The choice of space group of $P\bar{1}$ is based on the successful refinement of the structure. Details are given in Table 1 and in the Supporting Information.

X-ray-quality crystals of **16** were grown from toluene/hexane solution at −30 °C. A procedure similar to that of **1** was followed.. The structure was solved by direct methods. The choice of space group of $P2_1/n$ is based on systematic absence and the successful refinement of the structure. Details are given in Table 1 and in the Supporting Information.

(39) Stephenson, D. S.; Binsch, G. *DNMR5: Iterative Nuclear Magnetic Resonance Program for Unsaturated Exchange-Broadened Band-shapes*; *QCPE 11*, 365 ed.; Stephenson, D. S., Binsch, G., Eds.; Indiana University: Bloomington, IN, 1978.

Table 1. Crystal Data and Structure Refinement Parameters for Compounds **1**, **4**−**6**, **8**−**11**, **13**, **16**, and **17**

	1	**4**	**5**	**6**	**8**	**9**
empirical formula	$C_{28}H_{40}N_4O_2Zr$	$C_{28}H_{58}Cl_4N_2O_2Ti{\cdot}C_4H_8O$	$C_{25}H_{39}N_5Ti$	$C_{25}H_{39}N_5Zr$	$(C_{33}H_{53}ClN_4Zr)_2$	$C_{24}H_{28}Cl_2N_2O_2Ti$
fw	555.86	696.41	457.51	500.83	1264.93	495.28
space group	$P2_1/c$	$C2/c$	$P\bar{1}$	$P\bar{1}$	$P\bar{1}$	$Pbca$
a, Å	18.272(4)	15.260(3)	8.6972(1)	8.669(2)	12.3106(1)	11.5548(2)
b, Å	9.102(2)	16.724(3)	10.5162(1)	10.385(2)	16.8085(3)	20.0716(3)
c, Å	17.200(3)	27.774(6)	15.5363(1)	15.874(3)	17.5560(3)	21.5875(1)
α, deg			102.53	102.19(3)	87.0030(10)	
β, deg	98.15(3)	90.46(3)	93.59	92.92(3)	76.07	
γ, deg			102.519(1)	101.28(3)	77.997(1)	
V, Å^3	2831.5(1)	7088(3)	1345.12(2)	1363.5(5)	3448.82(9)	5006.64(12)
Z	4	8	2	2	2	8
temp, K	173(2)	133(2)	173(2)	173(2)	173(2)	132(2)
λ, Å	0.710 73	0.710 73	0.710 73	0.710 73	0.710 73	0.710 73
ρ(calc), g cm^{-3}	1.304	1.305	1.130	1.220	1.218	1.314
μ(Mo Kα), mm^{-1}	0.418	0.576	0.337	0.422	0.422	0.577
GOF[a]	0.987	1.052	0.921	0.300	0.836	1.094
R1 (all data)[b]	0.1500	0.1636	0.0466	0.0969	0.0696	0.1141
wR2[c]	0.1958	0.1313	0.1205	0.1527	0.1314	0.1086

	10	**11**	**13**	**16**	**17**
empirical formula	$C_{24}H_{28}Cl_2N_2O_2Zr$	$(C_{28}H_{36}Cl_2N_2O_2Ti){\cdot}CH_2Cl_2$	$(C_{19}H_{21}Cl_3N_2Ti){\cdot}C_7H_8$	$C_{38}H_{42}Cl_2N_4Zr$	$C_{29}H_{41}Cl_3N_2Zr$
fw	538.60	636.31	503.69	716.88	615.21
space group	$P3_121$	$P\bar{1}$	$P\bar{1}$	$P2_1/n$	$Pnma$
a, Å	8.6167(1)	8.1662(1)	7.286(2)	9.179(2)	14.054(3)
b, Å	8.6154(1)	14.8386(2)	13.154(3)	22.868(5)	21.842(4)
c, Å	28.5731(1)	14.9441(2)	15.253(3)	16.813(3)	9.856(2)
α, deg		67.1821(7)	103.25(3)		
β, deg		83.7061(7)	99.96(3)	98.77(3)	
γ, deg		77.7641(7)	94.58(3)		
V, Å^3	1836.98(3)	1630.46(4)	1390.6(5)	3487.9(12)	3025.6(11)
Z	3	2	2	4	4
temp, K	131(2)	132(2)	173(2)	173(2)	173(2)
λ, Å	0.710 73	0.710 69	0.710 73	0.710 73	0.710 73
ρ(calc), g cm^{-3}	1.461	1.296	1.203	1.365	1.351
μ(Mo Kα), mm^{-1}	0.690	0.617	0.609	0.501	0.648
GOF[a]	1.168	1.057	0.846	1.019	0.859
R1 (all data)[b]	0.0177	0.0394	0.1278	0.0571	0.0493
wR2[c]	0.0447	0.0891	0.2027	0.0770	0.1144

[a] GOF = $[\sum[w(F_o^2 - F_c^2)^2]/(n-p)]^{1/2}$, where *n* is the number of reflections and *p* the total number of parameters refined. [b] R1 = $\sum||F_o| - |F_c||/\sum|F_o|$. [c] wR2 = $[\sum[w(F_o^2 - F_c^2)^2]/\sum[w(F_o^2)^2]]^{1/2}$.

X-ray-quality crystals of **17** were grown from toluene/hexane solution at −30 °C. A procedure similar to that of **1** was followed. The structure was solved by direct methods. The choice of space group of *Pnma* is based on the systematic reflection absence and successful refinement of the structure. Details are given in Table 1 and in the Supporting Information.

Results

Three synthons are useful for introducing ketiminate ligands: the neutral ligand, iminium salts of the neutral ligand, and alkali metal ligand anions. For neutral and cationic ligands, ketiminateamido complexes can be prepared by amine elimination reactions from metal amides. Ketiminate halide compounds can be prepared from alkali ketiminates and metal halides. The following sections outline reactivity of group 4 compounds with reagents derived from the following mono- and diketimines shown in Chart 1: TolnacacH, MesnacacH, TolnacnacH, and DipnacnacH (TolnacacH = 4-*p*-toluidinopent-3-en-2-one, Mesnacac H = 4-(2,4,6-trimethylanilino)pent-3-en-2-one, Tolnacnac H = 2-(*p*-tolylamino)-4-(*p*-tolylimino)-2-pentene, Dipnacnac H = 2-((2,6-diisopropylphenyl)amino)-4-((2,6-diisopropylphenyl)imino)-2-pentene).

Reactions Involving Ketimines and Diketimines. $Ti(NMe_2)_4$ and $Zr(NMe_2)_4$ react cleanly with the ketimine, TolnacacH; however, the zirconium and titanium products differ significantly. For Zr, the ligand transfer proceeds smoothly with elimination of dimethylamine, and $(Tolnacac)_2Zr(NMe_2)_2$ (**1**) can be isolated in 66% yield (eq 1). The spectroscopic data indicate one tolyl environment but do not distinguish between potential stereoisomers for compound **1**. The structure of

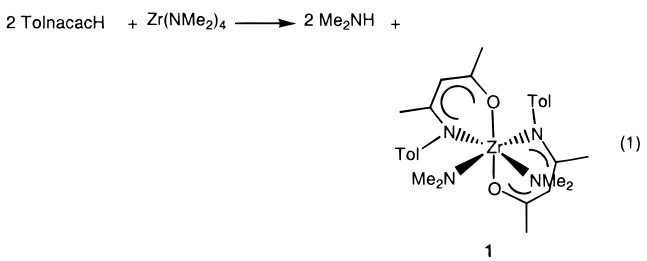

1

compound **1** was determined, yielding the connectivity in Figure 1. Table 1 summarizes crystal data and structure refinement parameters for the crystallographically characterized compounds in this paper. Selected bond distances and angles are listed in Table 2. The structure establishes cis disposition of the dimethylamide groups, cis coordination of the diketiminate N atoms, and trans disposition of the ketiminate O atoms. The reaction between $Zr(NMe_2)_4$ and 1 equiv of TolnacacH gives a mixture of compound **1** and $Zr(NMe_2)_4$.

The corresponding reaction of TolnacacH and $Ti(NMe_2)_4$ does not give the corresponding chelate complex. Instead, $[TiO_2]$ precipitates, dimethylamine is generated, and 2-(dimethylamino)-4-(*p*-tolylimino)-2-pentene (**2**) can be isolated from the

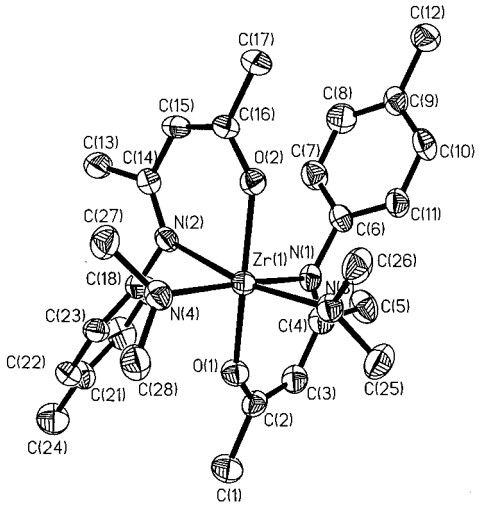

Figure 1. Structure of $(Tolnacac)_2Zr(NMe_2)_2$ (**1**). Thermal ellipsoids are drawn at 50% probability, and hydrogen positions are omitted for clarity.

Table 2. Selected Bond Distances and Angles for $(Tolnacac)_2Zr(NMe_2)_2$ (**1**)

Bond Lengths (Å)			
Zr(1)−O(2)	2.050(4)	N(1)−C(4)	1.317(7)
Zr(1)−O(1)	2.051(4)	N(1)−C(6)	1.440(7)
Zr(1)−N(4)	2.077(5)	C(1)−C(2)	1.496(8)
Zr(1)−N(3)	2.076(5)	C(2)−C(3)	1.361(8)
Zr(1)−N(1)	2.385(5)	C(3)−C(4)	1.435(8)
Zr(1)−N(2)	2.400(5)	C(4)−C(5)	1.512(8)
O(1)−C(2)	1.307(6)	C(13)−C(14)	1.521(8)
O(2)−C(16)	1.312(7)	C(14)−C(15)	1.435(7)
N(2)−C(14)	1.298(7)	C(15)−C(16)	1.368(8)
N(2)−C(18)	1.437(7)	C(16)−C(17)	1.498(7)
Bond Angles (deg)			
O(2)−Zr(1)−O(1)	164.0(2)	O(1)−Zr(1)−N(1)	76.4(2)
O(2)−Zr(1)−N(4)	95.7(2)	N(4)−Zr(1)−N(1)	164.7(2)
O(1)−Zr(1)−N(4)	94.7(2)	N(3)−Zr(1)−N(1)	88.9(2)
O(2)−Zr(1)−N(3)	94.5(2)	O(2)−Zr(1)−N(2)	77.0(2)
O(1)−Zr(1)−N(3)	94.6(2)	O(1)−Zr(1)−N(2)	91.6(2)
N(4)−Zr(1)−N(3)	104.4(2)	N(4)−Zr(1)−N(2)	86.3(2)
O(2)−Zr(1)−N(1)	90.7(2)	N(3)−Zr(1)−N(2)	167.1(2)
C(2)−O(1)−Zr(1)	142.2(4)	C(16)−O(2)−Zr(1)	141.2(4)
O(1)−C(2)−C(3)	122.8(5)	O(2)−C(16)−C(15)	123.0(5)
C(2)−C(3)−C(4)	126.2(5)	C(16)−C(15)−C(14)	126.2(6)
C(4)−N(1)−Zr(1)	129.9(4)	C(14)−N(2)−Zr(1)	128.8(4)

supernatant. The balanced reaction is shown in eq 2. Compound **2** was characterized using standard spectroscopic and analytical methods.

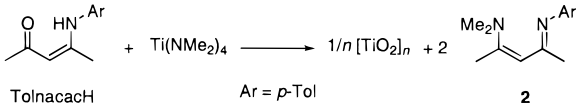

(2)

With less nucleophilic ligands on Ti, deoxygenation reactions are avoided and ketimine titanium complexes can be isolated. For example, TolnacacH reacts cleanly in a 2:1 molar ratio with $TiCl_4(thf)_2$ to give the coordination complex, $TiCl_4(TolnacacH)_2$ (**3**, eq 3). Due to its sparing solubility in thf, microcrystalline

$$2\ \text{TolnacacH} + \text{TiCl}_4(\text{thf})_2 \rightarrow 2\ \text{thf} + \underset{\mathbf{3}}{\textit{trans}\text{-}(\text{TolnacacH})_2\text{TiCl}_4} \qquad (3)$$

compound **3** can be isolated from the reaction mixture in 90% yield. The ^1H NMR spectrum shows a single set of ligand protons and a low-field resonance at δ 12.62 comparable to that for the N−H proton in TolnacacH (δ 12.40). Elemental

Table 3. Selected Bond Distances and Angles for *trans*-$(MesnacacH)_2TiCl_4$ (**4**)[a]

Bond Lengths (Å)			
Ti(1)−O(1)	1.915(3)	O(1)−C(2)	1.298(6)
Ti(1)−O(1A)	1.915(3)	C(1)−C(2)	1.501(7)
Ti(1)−Cl(2A)	2.321(2)	C(2)−C(3)	1.362(7)
Ti(1)−Cl(2)	2.321(2)	C(3)−C(4)	1.418(7)
Ti(1)−Cl(1)	2.353(2)	C(4)−N(1)	1.316(6)
Bond Angles (deg)			
O(1)−Ti(1)−O(1A)	175.5(2)	O(1)−Ti(1)−Cl(1A)	89.22(11)
O(1)−Ti(1)−Cl(2A)	89.98(12)	O(1A)−Ti(1)−Cl(1A)	87.58(11)
O(1A)−Ti(1)−Cl(2A)	93.17(11)	Cl(2A)−Ti(1)−Cl(1A)	178.88(7)
O(1)−Ti(1)−Cl(2)	93.17(11)	Cl(2)−Ti(1)−Cl(1A)	89.54(5)
O(1A)−Ti(1)−Cl(2)	89.98(12)	Cl(1)−Ti(1)−Cl(1A)	89.63(9)
Cl(2A)−Ti(1)−Cl(2)	91.29(10)	C(2)−O(1)−Ti(1)	155.7(3)
O(1)−Ti(1)−Cl(1)	87.58(11)	O(1)−C(2)−C(3)	121.9(5)
O(1A)−Ti(1)−Cl(1)	89.22(11)	C(2)−C(3)−C(4)	125.7(5)
Cl(2A)−Ti(1)−Cl(1)	89.55(5)	N(1)−C(4)−C(3)	122.2(5)

[a] Symmetry transformation used to generate equivalent atoms: A, $-x, y, -z + {}^1/_2$.

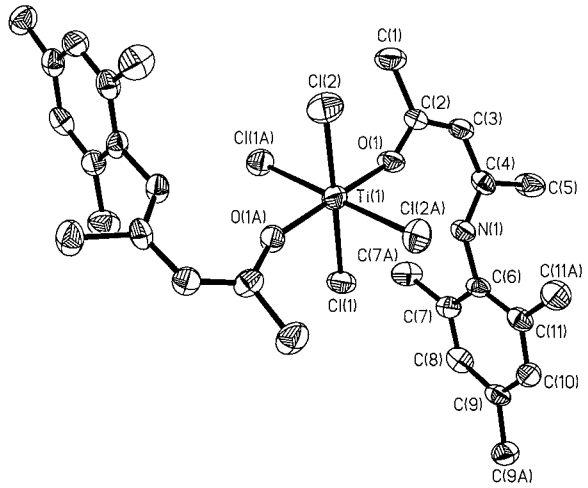

Figure 2. Structure of $TiCl_4(MesnacacH)_2(C_4H_8O)$ (**4**). One of two crystallographically independent molecules is displayed, and the thf solvate has been omitted. One-half of the molecule is generated by a 2-fold rotational axis. Thermal ellipsoids are drawn at 50% probability, and hydrogen positions are omitted for clarity.

analyses are consistent with formation of a bis(ketimine) $TiCl_4$ adduct, and the molecular structure of the homologue $TiCl_4(MesnacacH)_2$ (**4**) was solved. Table 3 lists selected bond distances and angles for compound **4**, and the structure is shown in Figure 2. The MesnacacH ligates in a monodentate fashion through the O atoms, which are trans. The titanium center is pseudooctahedral, and there are no significant contacts between titanium and the imine nitrogens. The position of the acidic proton remains ambiguous since imine H atoms could not be located from difference maps and we have not prepared ^{15}N derivatives to evaluate perturbations in $|^1J_{NH}|$. Corresponding reactions of diketiminate ligands with $TiCl_4(thf)_2$ and $ZrCl_4(thf)_2$, and ketiminate ligands with $ZrCl_4(thf)_2$, do not yield tractable products.

In chemistry analogous to that reported by Collins, TolnacnacH reacts cleanly in 1:1 molar ratios with $Zr(NMe)_4$ and $Ti(NMe_2)_4$ to afford the five-coordinate complexes $(Tolnacnac)M(NMe_2)_3$ (eq 4, M = Ti, **5**, 87% yield; M = Zr, **6**, 98% yield).[25]

$$\text{TolnacnacH} + \text{M(NMe}_2)_4 \rightarrow \text{Me}_2\text{NH} + \underset{\text{M = Ti (}\mathbf{5}\text{), Zr (}\mathbf{6}\text{)}}{(\text{Tolnacnac})\text{M(NMe}_2)_3} \qquad (4)$$

$$2\ \text{TolnacnacH} + \text{Zr(NMe}_2)_4 \rightarrow 2\ \text{Me}_2\text{NH} + \underset{\mathbf{7}}{(\text{Tolnacnac})_2\text{Zr(NMe}_2)_2} \qquad (5)$$

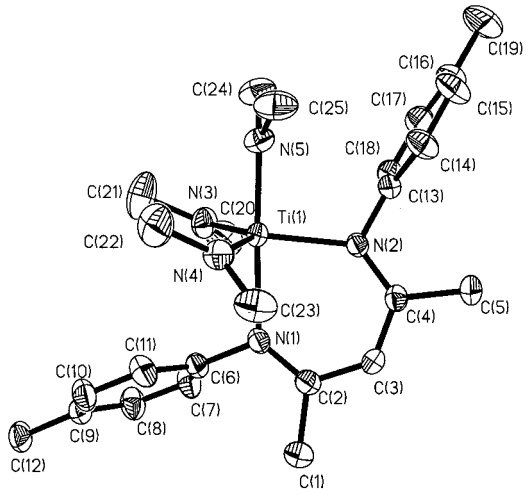

Figure 3. Structures of (Tolnacnac)Ti(NMe_2)$_3$ (**5**). Thermal ellipsoids are drawn at 50% probability, and hydrogen positions are omitted for clarity.

The zirconium compound undergoes a second aminolysis to generate (Tolnacnac)$_2$Zr(NMe_2)$_2$ (**7**, eq 5) at elevated temperature, but (Tolnacnac)Ti(NMe_2)$_3$ does not react cleanly with a second equiv of TolnacnacH. For compound **7**, two sets of Tolnacnac methyl resonances are observed by NMR spectroscopy, and chemical exchange between these resonances was not detected at elevated temperatures. This contrasts behavior of halide and alkoxide bis(diketiminate) derivatives (vide infra) where isomerization is rapid on the NMR time scale. The more hindered diketimine, DipnacnacH, does not give analogous products when reacted with Zr(NMe_2)$_4$ or Ti(NMe_2)$_4$ in refluxing toluene.

Since structures of (L)M(NMe_2)$_3$ derivatives (where L is a diketiminate ligand) have not been reported, the structures for compounds **5** and **6** were determined. Since the Ti and Zr complexes are similar, only the Ti structure is shown in Figure 3. Selected bond distances and bond angles for both complexes are listed in Table 4. The structure in Figure 3 has a trigonal bipyramidal geometry with the diketiminate N atoms occupying axial and equatorial positions. For the diketiminate ligand, the M−N axial distance is significantly longer than M−N basal distance in titanium and zirconium derivatives.

VT ^{1}H NMR experiments for compounds **5** and **6** have been performed in C_7D_8. For the zirconium compound, single sets of diketiminate and dimethylamide environments are observed between −80 °C and 25 °C. For the titanium compound, the diketiminate and dimethylamide resonances start to decoalesce at −60 °C. Two chemically distinct environments are observed for the methyl resonances at ligand backbone and tolyl positions at −80 °C. The dimethylamide resonance decoalesces to three equal intensity resonances for the six methyl groups.

Reactivity of DipnacnacH·HCl with Zr(NMe)$_4$. Addition of Zr(NMe_2)$_4$ to a toluene suspension of DipnacnacH·HCl gives a homogeneous solution from which (Dipnacnac)ZrCl(NMe_2)$_2$ (**8**) is isolated in 51% yield (eq 6). At room temperature, the

$$\text{DipnacnacH·HCl} + \text{Zr}(\text{NMe}_2)_4 \rightarrow 2\ \text{Me}_2\text{NH} + \underset{\mathbf{8}}{(\text{Dipnacnac})\text{ZrCl}(\text{NMe}_2)_2} \quad (6)$$

^{1}H NMR spectrum of compound **8** is broad and featureless. Above 50 °C, a single N*Me*$_2$ (δ 2.70) resonance in the ^{1}H NMR spectrum indicates a fluxional structure. The molecular structure of compound **8** was determined to establish the coordination at Zr. Selected metrical data are included in Table 5, and the structure is shown in Figure 4. In contrast to compound **6**, the coordination geometry at zirconium is better described as square pyramidal with an NMe_2 ligand in the apical position.

Table 4. Selected Bond Distances and Angles for (Tolnacnac)Ti(NMe_2)$_3$ (**5**) and (Tolnacnac)Zr(NMe_2)$_3$ (**6**)

(Tolnacnac)Ti(NMe_2)$_3$ (**5**)		(Tolnacnac)Zr(NMe_2)$_3$ (**6**)	
	Bond Lengths (Å)		
Ti(1)−N(3)	1.909(2)	Zr(1)−N(3)	2.019(4)
Ti(1)−N(4)	1.919(2)	Zr(1)−N(4)	2.031(4)
Ti(1)−N(5)	1.962(2)	Zr(1)−N(5)	2.071(4)
Ti(1)−N(2)	2.090(2)	Zr(1)−N(2)	2.211(4)
Ti(1)−N(1)	2.237(2)	Zr(1)−N(1)	2.350(4)
N(1)−C(2)	1.322(3)	N(1)−C(2)	1.323(6)
N(1)−C(6)	1.448(2)	N(1)−C(6)	1.454(6)
C(2)−C(3)	1.423(3)	C(2)−C(3)	1.402(7)
C(4)−C(3)	1.384(3)	C(3)−C(4)	1.381(7)
N(2)−C(4)	1.354(2)	N(2)−C(4)	1.348(6)
N(2)−C(13)	1.448(2)	N(2)−C(13)	1.453(6)
	Bond Angles (deg)		
N(3)−Ti(1)−N(4)	121.27(8)	N(3)−Zr(1)−N(4)	120.5(2)
N(3)−Ti(1)−N(5)	92.75(8)	N(3)−Zr(1)−N(5)	94.5(2)
N(4)−Ti(1)−N(5)	91.50(7)	N(4)−Zr(1)−N(5)	91.6(2)
N(3)−Ti(1)−N(2)	119.40(7)	N(3)−Zr(1)−N(2)	118.4(2)
N(4)−Ti(1)−N(2)	118.35(7)	N(4)−Zr(1)−N(2)	119.8(2)
N(5)−Ti(1)−N(2)	95.63(7)	N(5)−Zr(1)−N(2)	95.0(2)
N(3)−Ti(1)−N(1)	89.53(7)	N(3)−Zr(1)−N(1)	92.3(2)
N(4)−Ti(1)−N(1)	88.27(7)	N(4)−Zr(1)−N(1)	88.2(2)
N(5)−Ti(1)−N(1)	177.46(6)	N(5)−Zr(1)−N(1)	172.13(14)
N(1)−Ti(1)−N(2)	82.32(5)	N(1)−Zr(1)−N(2)	78.28(14)
C(21)−N(3)−C(20)	112.1(2)	C(20)−N(3)−C(21)	112.0(5)
C(21)−N(3)−Ti(1)	124.4(2)	C(20)−N(3)−Zr(1)	126.5(4)
C(20)−N(3)−Ti(1)	123.5(2)	C(21)−N(3)−Zr(1)	121.3(4)
C(22)−N(4)−C(23)	112.6(2)	C(22)−N(4)−C(23)	113.8(5)
C(22)−N(4)−Ti(1)	129.4(2)	C(22)−N(4)−Zr(1)	132.0(4)
C(23)−N(4)−Ti(1)	117.95(14)	C(23)−N(4)−Zr(1)	114.1(4)
C(24)−N(5)−C(25)	109.0(2)	C(24)−N(5)−C(25)	107.6(4)
C(24)−N(5)−Ti(1)	125.04(14)	C(24)−N(5)−Zr(1)	127.9(3)
C(25)−N(5)−Ti(1)	125.15(14)	C(25)−N(5)−Zr(1)	123.8(3)
C(2)−N(1)−Ti(1)	128.05(12)	C(2)−N(1)−Zr(1)	128.3(3)
N(1)−C(2)−C(3)	121.8(2)	N(1)−C(2)−C(3)	122.0(4)
C(4)−C(3)−C(2)	127.6(2)	C(4)−C(3)−C(2)	129.4(5)
N(2)−C(4)−C(5)	119.3(2)	N(2)−C(4)−C(5)	119.7(4)
C(4)−N(2)−Ti(1)	129.09(12)	C(4)−N(2)−Zr(1)	129.8(3)

Table 5. Selected Bond Distances and Angles for (Dipnacnac)ZrCl(NMe_2)$_2$ (**8**)

	Bond Lengths (Å)		
Zr(1)−N(4)	2.014(2)	N(1)−C(2)	1.342(3)
Zr(1)−N(3)	2.052(2)	N(1)−C(6)	1.463(4)
Zr(1)−N(2)	2.249(2)	C(2)−C(3)	1.412(4)
Zr(1)−N(1)	2.319(2)	C(3)−C(4)	1.387(4)
Zr(1)−Cl(1)	2.4776(8)	N(2)−C(4)	1.358(3)
	Bond Angles (deg)		
N(4)−Zr(1)−N(3)	107.28(11)	C(2)−N(1)−Zr(1)	125.8(2)
N(4)−Zr(1)−N(2)	101.97(9)	N(1)−C(2)−C(3)	124.3(2)
N(3)−Zr(1)−N(2)	93.92(9)	C(4)−C(3)−C(2)	128.6(2)
N(4)−Zr(1)−N(1)	103.77(9)	N(2)−C(4)−C(3)	124.3(2)
N(3)−Zr(1)−N(1)	148.94(10)	C(4)−N(2)−Zr(1)	127.1(2)
N(2)−Zr(1)−N(1)	80.61(8)	C(30)−N(3)−C(31)	110.7(3)
N(4)−Zr(1)−Cl(1)	104.61(7)	C(30)−N(3)−Zr(1)	128.8(2)
N(3)−Zr(1)−Cl(1)	86.57(8)	C(31)−N(3)−Zr(1)	120.3(2)
N(2)−Zr(1)−Cl(1)	151.99(6)	C(33)−N(4)−C(32)	111.8(3)
N(1)−Zr(1)−Cl(1)	84.63(6)	C(33)−N(4)−Zr(1)	124.5(2)

Reactivity of Lithium Ketiminate and Diketiminate Complexes with Metal Halides. Lithium reagents for delivering ketiminate and diketiminate anions can be prepared in high yield from the neutral ligands and *n*-BuLi. In this section reactions of monoketiminate and diketiminate reagents with group 4 halide complexes are described.

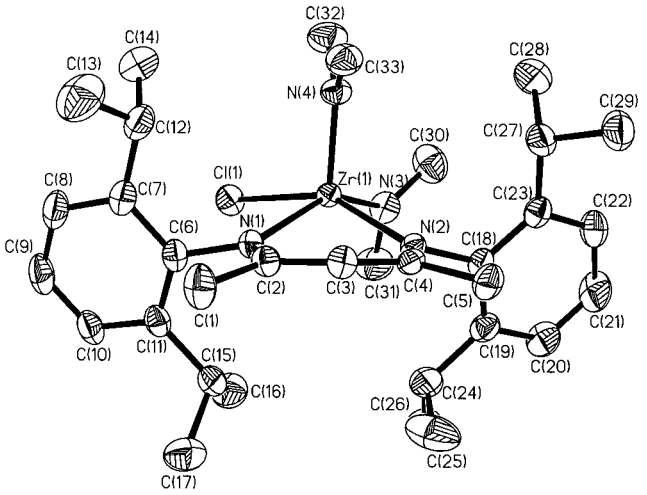

Figure 4. Structure of $[(Dipnacnac)ZrCl(NMe_2)_2]_2$ (**8**), displaying one of the two crystallographically independent molecules. Thermal ellipsoids are drawn at 50% probability, and hydrogen positions are omitted for clarity.

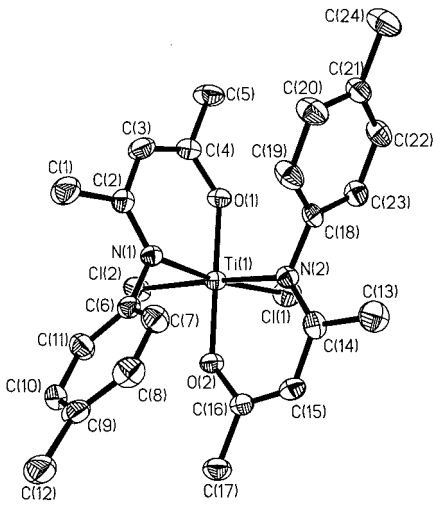

Figure 5. Structure of $(Tolnacac)_2TiCl_2$ (**9**). Thermal ellipsoids are drawn at 50% probability, and hydrogen positions are omitted for clarity.

Li(Tolnacac) reacts cleanly with $MCl_4(thf)_2$ (M = Ti, Zr) in 2:1 molar ratios to give the compounds $(Tolnacac)_2MCl_2$ (eq 7, M = Ti, **9**, 95% yield; M = Zr, **10**, 79% yield). In each case

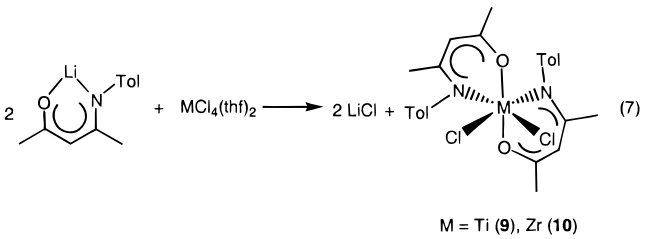

M = Ti (**9**), Zr (**10**)

a single set of methyl resonances for the ligand backbone and tolyl methyl groups is observed. ^1H and ^{13}C NMR data show that rotation about the aryl N−C bonds is slow on the NMR time scale. This is most clearly demonstrated by the observation of six aromatic resonances in the ^{13}C NMR spectra for these compounds. The Mesnacac analogues, $(Mesnacac)_2MCl_2$, have been similarly prepared (M = Ti, **11**, 70% yield; M = Zr, **12**, 79% yield). The NMR data for these complexes are similar to those for compounds **9** and **10**, and the observation of three mesityl methyl resonances in ^1H NMR spectra confirms slow aryl N−C bond rotation on the NMR time scale for compounds **11** and **12**.

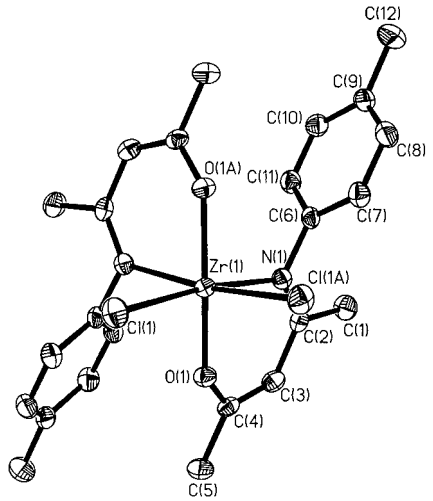

Figure 6. Structure of $(Tolnacac)_2ZrCl_2$ (**10**). Thermal ellipsoids are drawn at 50% probability, and hydrogen positions are omitted for clarity.

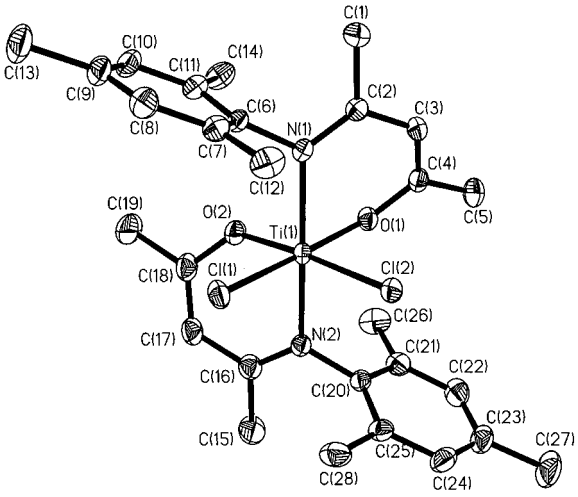

Figure 7. Structure of $[(Mesnacac)_2TiCl_2](CH_2Cl_2)$ (**11**) with thermal ellipsoids drawn at 50% probability. The methylene chloride solvate hydrogen positions are omitted for clarity.

Assignment of stereochemistry in compounds **9**−**12** cannot be made from the spectroscopic data. Thus, structural determinations were attempted in each case. Suitable single crystals were obtained for compounds **9**−**11**, and structures are shown in Figures 5−7, respectively. Selected bond distances and angles are listed in Tables 6 and 7. In all structures, the chlorides are cis. The major difference in the Tolnacac and Mesnacac complexes is the ketiminate orientation. For the Tolnacac complexes, **9** and **10**, the O and N atoms are trans and cis, respectively, whereas this orientation in compound **11** is reversed.[40,41]

Li(Tolnacnac) also reacts smoothly with $TiCl_4$ in 1:1 molar ratios to give diketiminate trichloride complex, (Tolnacnac)-

(40) de Angelis, S.; Solari, E.; Gallo, E.; Floriani, C.; Chiesi-Villa, A.; Rizzoli, C. *Inorg. Chem.* **1992**, *31*, 2520−2527.
(41) Corazza, F.; Solari, E.; Floriani, C.; Chiesi-Villa, A.; Guastini, C. *J. Chem. Soc., Dalton Trans.* **1990**, 1335−1344.

Table 6. Selected Bond Distances and Angles for $(Tolnacac)_2TiCl_2$ (**9**) and $(Tolnacac)_2ZrCl_2$ (**10**)

$(Tolnacac)_2TiCl_2$ (**9**)		$(Tolnacac)_2ZrCl_2$ (**10**)	
Bond Lengths (Å)			
Ti(1)−O(2)	1.892(2)	Zr(1)−O(1)	2.0120(10)
Ti(1)−O(1)	1.893(2)	Zr(1)−O(1A)	2.0120(10)
Ti(1)−N(1)	2.169(2)	Zr(1)−N(1)	2.3376(12)
Ti(1)−N(2)	2.171(2)	Zr(1)−N(1A)	2.3376(12)
Ti(1)−Cl(1)	2.3222(9)	Zr(1)−Cl(1)	2.4559(4)
Ti(1)−Cl(2)	2.3267(8)	Zr(1)−Cl(1A)	2.4559(4)
O(1)−C(4)	1.319(3)	O(1)−C(4)	1.318(2)
C(4)−C(3)	1.361(4)	C(3)−C(4)	1.358(2)
C(3)−C(2)	1.431(4)	C(2)−C(3)	1.436(2)
C(2)−N(1)	1.328(3)	C(2)−N(1)	1.322(2)
N(1)−C(6)	1.456(3)	N(1)−C(6)	1.449(2)
Bond Angles (deg)			
O(2)−Ti(1)−O(1)	170.74(8)	O(1)−Zr(1)−O(1A)	157.28(6)
O(2)−Ti(1)−N(1)	90.38(8)	O(1)−Zr(1)−N(1)	77.92(4)
O(1)−Ti(1)−N(1)	82.68(8)	O(1A)−Zr(1)−N(1)	86.16(5)
O(2)−Ti(1)−N(2)	82.92(8)	O(1)−Zr(1)−N(1A)	86.17(5)
O(1)−Ti(1)−N(2)	90.41(8)	O(1A)−Zr(1)−N(1A)	77.91(4)
N(1)−Ti(1)−N(2)	85.62(8)	N(1)−Zr(1)−N(1A)	90.96(6)
O(2)−Ti(1)−Cl(1)	94.99(6)	O(1)−Zr(1)−Cl(1)	95.14(3)
O(1)−Ti(1)−Cl(1)	91.14(6)	O(1A)−Zr(1)−Cl(1)	100.72(3)
N(1)−Ti(1)−Cl(1)	170.85(6)	N(1)−Zr(1)−Cl(1)	173.01(4)
N(2)−Ti(1)−Cl(1)	87.70(6)	N(1A)−Zr(1)−Cl(1)	89.33(3)
O(2)−Ti(1)−Cl(2)	92.37(6)	O(1)−Zr(1)−Cl(1A)	100.71(3)
O(1)−Ti(1)−Cl(2)	93.59(6)	O(1A)−Zr(1)−Cl(1A)	95.14(3)
N(1)−Ti(1)−Cl(2)	88.70(6)	N(1)−Zr(1)−Cl(1A)	89.33(3)
N(2)−Ti(1)−Cl(2)	172.58(6)	N(1A)−Zr(1)−Cl(1A)	173.01(4)
Cl(1)−Ti(1)−Cl(2)	98.45(3)	Cl(1)−Zr(1)−Cl(1A)	91.24(2)
C(4)−O(1)−Ti(1)	138.3(2)	C(4)−O(1)−Zr(1)	142.00(10)
O(1)−C(4)−C(3)	121.9(2)	O(1)−C(4)−C(3)	121.56(14)
C(4)−C(3)−C(2)	124.7(3)	C(4)−C(3)−C(2)	126.15(14)
N(1)−C(2)−C(3)	122.7(2)	N(1)−C(2)−C(3)	123.22(13)
C(2)−N(1)−Ti(1)	126.9(2)	C(2)−N(1)−Zr(1)	128.62(11)

[a] Symmetry transformations used to generate equivalent atoms: A, $x - y + 1, -y + 2, -z + {}^5/_3$.

$TiCl_3$ (**13**, eq 8), in 84% yield as maroon crystals. The reaction with $ZrCl_4(thf)_2$ gives the thf adduct, (Dipnacnac)$ZrCl_3$(thf) (**14**, eq 9), in 49% yield. We attempted to remove the coordinated

$$\text{Li(Tolnacnac)} + \text{TiCl}_4 \rightarrow \underset{\mathbf{13}}{\text{(Tolnacnac)TiCl}_3} + \text{LiCl} \qquad (8)$$

$$\text{Li(Dipnacnac)} + \text{ZrCl}_4(\text{thf})_2 \rightarrow \underset{\mathbf{14}}{\text{(Dipnacnac)ZrCl}_3(\text{thf})} + \text{thf} + \text{LiCl} \qquad (9)$$

thf in **14**. A toluene solution of compound **14** was heated to ~90 °C, and all volatile materials were slowly removed under vacuum. The ^{1}H NMR spectrum indicated that the thf remained intact.

The molecular structure of compound **13** was determined. Selected bond distances and angles are listed in Table 8, and the structure is shown in Figure 8. In this compound, an η^5-interaction between the Tolnacnac ligand and the titanium center is apparent. While the Tolnacnac ligand is distorted with relatively short Ti−N distances, the Ti−C distances are only slightly longer than those in pentadienyl structures. In contrast to other structures in this paper, the Tolnacnac backbone is nonplanar with C(3) displaced by 0.319 Å from the least-squares plane defined by N(1), N(2), C(2), and C(4). Presumably, the zirconium analogue, compound **15**, prepared by reacting compound **6** with excess $SiMe_3Cl$ or $CHCl_3$, adopts a similar structure. The resonance for the methine proton in (Tolnacnac)-MCl_3 (M = Ti, **13**, δ 6.03; M = Zr, **15**, δ 5.95) is shifted to substantially lower field in ^{1}H NMR compared to bona fide η^2-compounds (δ 5.0−5.4).

Table 7. Selected Bond Distances and Angles for $(Mesnacac)_2TiCl_2$ (**11**) and $(Tolnacnac)_2ZrCl_2$ (**16**)

$(Mesnacac)_2TiCl_2$ (**11**)		$(Tolnacnac)_2ZrCl_2$ (**16**)	
Bond Lengths (Å)			
Ti(1)−O(1)	1.8874(10)	Zr(1)−N(2)	2.197(2)
Ti(1)−O(2)	1.8902(10)	Zr(1)−N(3)	2.214(2)
Ti(1)−N(1)	2.1745(12)	Zr(1)−N(1)	2.243(2)
Ti(1)−N(2)	2.1764(12)	Zr(1)−N(4)	2.272(2)
Ti(1)−Cl(1)	2.3401(4)	Zr(1)−Cl(1)	2.4312(7)
Ti(1)−Cl(2)	2.3760(4)	Zr(1)−Cl(2)	2.4426(7)
N(1)−C(6)	1.456(2)	N(1)−C(6)	1.456(2)
N(1)−C(2)	1.327(2)	N(1)−C(2)	1.336(3)
C(2)−C(3)	1.437(2)	C(2)−C(3)	1.406(3)
C(3)−C(4)	1.369(2)	C(3)−C(4)	1.390(3)
C(4)−O(1)	1.327(2)	N(2)−C(4)	1.330(3)
N(2)−C(20)	1.453(2)	N(3)−C(25)	1.444(3)
N(2)−C(16)	1.321(2)	N(3)−C(21)	1.334(3)
C(16)−C(17)	1.435(2)	C(21)−C(22)	1.389(3)
C(17)−C(18)	1.363(2)	C(22)−C(23)	1.404(3)
C(18)−O(2)	1.331(2)	N(4)−C(23)	1.339(3)
Bond Angles (deg)			
O(1)−Ti(1)−O(2)	94.51(5)	N(2)−Zr(1)−N(3)	157.65(6)
O(1)−Ti(1)−N(1)	82.40(4)	N(2)−Zr(1)−N(1)	79.31(7)
O(2)−Ti(1)−N(1)	92.32(4)	N(3)−Zr(1)−N(1)	87.49(6)
O(1)−Ti(1)−N(2)	93.18(4)	N(2)−Zr(1)−N(4)	83.19(6)
O(2)−Ti(1)−N(2)	82.52(5)	N(3)−Zr(1)−N(4)	78.52(6)
N(1)−Ti(1)−N(2)	172.95(5)	N(1)−Zr(1)−N(4)	88.72(6)
O(1)−Ti(1)−Cl(1)	174.59(3)	N(2)−Zr(1)−Cl(1)	99.64(5)
O(2)−Ti(1)−Cl(1)	89.25(4)	N(3)−Zr(1)−Cl(1)	97.67(5)
N(1)−Ti(1)−Cl(1)	93.59(3)	N(1)−Zr(1)−Cl(1)	87.39(5)
N(2)−Ti(1)−Cl(1)	91.15(3)	N(4)−Zr(1)−Cl(1)	174.67(4)
O(1)−Ti(1)−Cl(2)	87.48(3)	N(2)−Zr(1)−Cl(2)	98.70(5)
O(2)−Ti(1)−Cl(2)	175.96(4)	N(3)−Zr(1)−Cl(2)	95.28(5)
N(1)−Ti(1)−Cl(2)	91.42(3)	N(1)−Zr(1)−Cl(2)	176.51(5)
N(2)−Ti(1)−Cl(2)	93.87(3)	N(4)−Zr(1)−Cl(2)	93.91(5)
Cl(1)−Ti(1)−Cl(2)	89.01(2)	Cl(1)−Zr(1)−Cl(2)	90.13(3)
C(2)−N(1)−Ti(1)	123.99(9)	C(2)−N(1)−Zr(1)	122.64(13)
N(1)−C(2)−C(3)	122.72(13)	N(1)−C(2)−C(3)	123.1(2)
C(4)−C(3)−C(2)	123.99(13)	C(4)−C(3)−C(2)	126.6(2)
O(1)−C(4)−C(3)	121.10(13)	N(2)−C(4)−C(3)	122.2(2)
C(4)−O(1)−Ti(1)	131.58(9)	C(4)−N(2)−Zr(1)	127.18(14)
C(16)−N(2)−Ti(1)	123.94(10)	C(21)−N(3)−Zr(1)	126.79(14)
N(2)−C(16)−C(17)	122.79(14)	N(3)−C(21)−C(22)	122.4(2)
C(18)−C(17)−C(16)	123.94(14)	C(21)−C(22)−C(23)	126.9(2)
O(2)−C(18)−C(17)	121.56(14)	N(4)−C(23)−C(22)	122.4(2)
C(18)−O(2)−Ti(1)	130.77(10)	C(23)−N(4)−Zr(1)	122.61(13)

$ZrCl_4(thf)_2$ reacted cleanly with 2 equiv of Li(Tolnacnac) to yield *cis*-$(Tolnacnac)_2ZrCl_2$ (**16**, eq 10) in 50% yield. ^{1}H NMR

$$2\ \text{Li(Tolnacnac)} + \text{ZrCl}_4(\text{thf})_2 \rightarrow \underset{\mathbf{16}}{\text{(Tolnacnac)}_2\text{ZrCl}_2} + 2\ \text{thf} + 2\ \text{LiCl} \qquad (10)$$

data for this complex indicate equivalent methyl environments for the tolyl and ligand methyl groups at room temperature. Upon cooling, these resonances decoalesce and activation parameters for this fluxional process could be extracted from full line-shape analysis ($\Delta H^{\ddagger} = 9(1)$ kcal/mol, $\Delta S^{\ddagger} = -13(4)$ eu) using DNMR5 (Table 10).[39] The structure of compound **16** was determined. Selected bond lengths and angles are listed in Table 7, and the structure is depicted in Figure 9. The cis orientation of the chlorides is consistent with the low-temperature NMR data.

The addition of Li(Dipnacnac) to a slurry of $ZrCl_4$ in toluene gives the base-free complex, (Dipnacnac)$ZrCl_3$ (**17**, eq 11), in

$$\text{Li(Dipnacnac)} + \text{ZrCl}_4 \rightarrow \underset{\mathbf{17}}{\text{(Dipnacnac)ZrCl}_3} + 2\ \text{LiCl} \qquad (11)$$

57% yield. The molecular structure for this compound was determined. Selected bond distances and angles are listed in

Table 8. Selected Bond Distances and Angles for (Tolnacnac)$TiCl_3$ (**13**)

Bond Lengths (Å)			
Ti(1)−N(2)	1.995(4)	N(1)−C(2)	1.324(6)
Ti(1)−N(1)	1.995(4)	N(1)−C(6)	1.441(6)
Ti(1)−Cl(1)	2.218(2)	N(2)−C(4)	1.331(5)
Ti(1)−Cl(3)	2.335(2)	N(2)−C(13)	1.439(6)
Ti(1)−Cl(2)	2.337(2)	C(1)−C(2)	1.51(2)
Ti(1)−C(3)	2.535(4)	C(2)−C(3)	1.419(7)
Ti(1)−C(4)	2.535(5)	C(3)−C(4)	1.416(7)
Ti(1)−C(2)	2.559(5)	C(6)−C(7)	1.392(7)
Bond Angles (deg)			
N(2)−Ti(1)−N(1)	85.1(2)	N(2)−Ti(1)−C(4)	31.4(2)
N(2)−Ti(1)−Cl(1)	95.38(12)	N(1)−Ti(1)−C(4)	78.8(2)
N(1)−Ti(1)−Cl(1)	99.29(12)	Cl(1)−Ti(1)−C(4)	126.65(12)
N(2)−Ti(1)−Cl(3)	162.77(12)	Cl(3)−Ti(1)−C(4)	131.39(12)
N(1)−Ti(1)−Cl(3)	91.27(13)	Cl(2)−Ti(1)−C(4)	80.82(11)
Cl(1)−Ti(1)−Cl(3)	101.83(6)	C(3)−Ti(1)−C(4)	32.4(2)
N(2)−Ti(1)−Cl(2)	87.25(12)	N(2)−Ti(1)−C(2)	79.1(2)
N(1)−Ti(1)−Cl(2)	152.34(12)	N(1)−Ti(1)−C(2)	30.8(2)
Cl(1)−Ti(1)−Cl(2)	107.87(6)	Cl(1)−Ti(1)−C(2)	129.63(12)
Cl(3)−Ti(1)−Cl(2)	88.27(7)	Cl(3)−Ti(1)−C(2)	89.16(13)
N(2)−Ti(1)−C(3)	61.6(2)	Cl(2)−Ti(1)−C(2)	121.61(11)
N(1)−Ti(1)−C(3)	61.0(2)	C(3)−Ti(1)−C(2)	32.3(2)
Cl(1)−Ti(1)−C(3)	149.21(13)	C(4)−Ti(1)−C(2)	58.9(2)
Cl(3)−Ti(1)−C(3)	101.98(13)	C(2)−N(1)−C(6)	121.7(4)
Cl(2)−Ti(1)−C(3)	92.08(12)	C(2)−N(1)−Ti(1)	98.9(3)
N(1)−C(2)−C(3)	117.4(4)	N(2)−C(4)−C(3)	118.9(4)
N(1)−C(2)−Ti(1)	50.3(2)	N(2)−C(4)−Ti(1)	51.3(2)
C(4)−C(3)−C(2)	124.3(4)	C(3)−C(4)−Ti(1)	73.8(3)
C(4)−C(3)−Ti(1)	73.8(3)	C(4)−N(2)−C(13)	122.2(4)
C(2)−C(3)−Ti(1)	74.8(3)	C(4)−N(2)−Ti(1)	97.3(3)

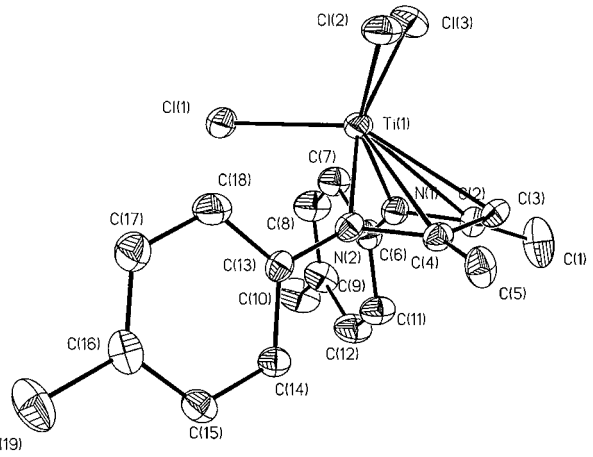

Figure 8. Structure of [(Tolnacnac)$TiCl_3$](C_7H_8) (**13**) with thermal ellipsoids drawn at 50% probability. The toluene solvate and hydrogen positions are omitted for clarity.

Table 9, and the structure is shown in Figure 10. There is a crystallographic mirror plane containing Zr(1), Cl(2), and C(3). In contrast to the structure for compound **13**, the Dipnacnac ligand binds in η^2-fashion (Zr(1)−N(1), 2.202(2) Å; Zr(1)−N(1A), 2.202(2) Å) and the geometry about zirconium is best described as square pyramidal with Cl(2) occupying an axial position. The Zr−Cl(2) bond distance (Zr(1)−Cl(2), 2.3392(9) Å) is only slightly shorter than the equatorial Zr−Cl distances (Zr(1)−Cl(1), 2.3945(7) Å; Zr(1)−Cl(1A), 2.3945(7) Å). To minimize the interaction between ^{i}Pr groups with Cl(1) and Cl(1A), the ligand backbone plane N(1), N(1A), C(2), C(3) is almost parallel with the basal plane Cl(1), Cl(1A), N(1), N(1A). Attempts to prepare compound **15** via this route gave mixtures of compounds **15** and **16**.

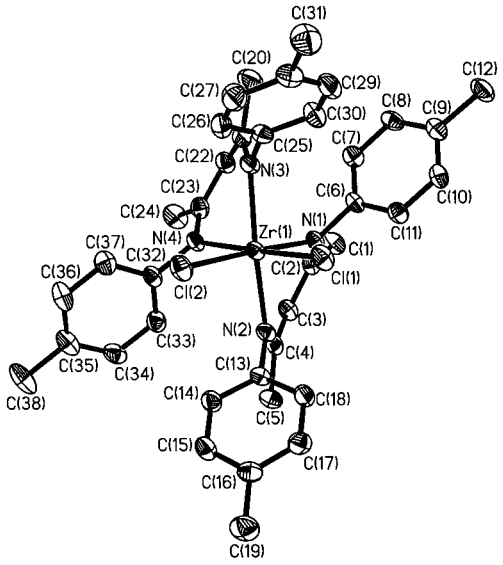

Figure 9. Structure of (Tolnacnac)$_2ZrCl_2$ (**16**). Thermal ellipsoids are drawn at 50% probability, and hydrogen positions are omitted for clarity.

Table 9. Selected Bond Distances and Angles for (Dipnacnac)$ZrCl_3$ (**17**)[a]

Bond Lengths (Å)			
Zr(1)−N(1A)	2.202(2)	Zr(1)−Cl(1)	2.3945(7)
Zr(1)−N(1)	2.202(2)	Zr(1)−Cl(1A)	2.3945(7)
Zr(1)−Cl(2)	2.3392(9)	N(1)−C(2)	1.352(2)
N(1)−C(2)	1.352(2)	C(2)−C(3)	1.391(2)
Bond Angles (deg)			
N(1A)−Zr(1)−N(1)	83.64(8)	Cl(2)−Zr(1)−Cl(1)	107.86(3)
N(1A)−Zr(1)−Cl(2)	102.54(5)	N(1A)−Zr(1)−Cl(1A)	86.97(4)
N(1)−Zr(1)−Cl(2)	102.54(5)	N(1)−Zr(1)−Cl(1A)	149.46(5)
N(1A)−Zr(1)−Cl(1)	149.45(5)	Cl(2)−Zr(1)−Cl(1A)	107.86(3)
N(1)−Zr(1)−Cl(1)	86.97(4)	Cl(1)−Zr(1)−Cl(1A)	86.54(4)
C(2)−N(1)−Zr(1)	123.33(12)	C(2)−C(3)−C(2A)	129.0(2)
N(1)−C(2)−C(3)	124.0(2)	C(3)−C(2)−C(1)	116.0(2)

[a] Symmetry transformations used to generate equivalent atoms: A, $x, -y + {}^1/_2, z$.

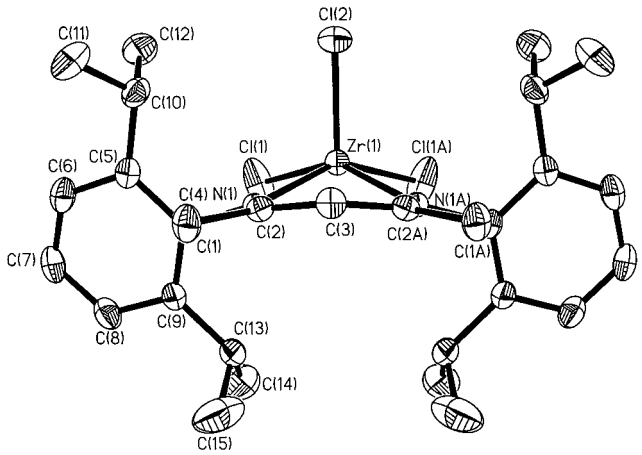

Figure 10. Structure of (Dipnacnac)$ZrCl_3$ (**17**). Thermal ellipsoids are drawn at 50% probability, and hydrogen positions are omitted for clarity.

Aminolysis Reactions of Compounds 6 and 7 with Alcohols. When the zirconium amide complexes **6** and **7** are treated with stoichiometric amounts of alcohols, alkoxide complexes can be isolated. Zirconium tris(amide) **6** reacts with 3 equiv of MeOH to yield (Tolnacnac)$Zr(OMe)_3$ (eq 12, **18**) in 9% yield.

The major side product is TolnacnacH. $(Tolnacnac)_2Zr(OMe)_2$ (eq 13, **19**) can be prepared from zirconium bis(amide) **7** and 2

$$\underset{\mathbf{6}}{(Tolnacnac)Zr(NMe_2)_3} + 3\ MeOH \rightarrow \underset{\mathbf{18}}{(Tolnacnac)Zr(OMe)_3} + 3\ HNMe_2 \quad (12)$$

$$\underset{\mathbf{7}}{(Tolnacnac)_2Zr(NMe_2)_2} + 2\ MeOH \rightarrow \underset{\mathbf{20}}{(Tolnacnac)_2Zr(OMe)_2} + 2\ HNMe_2 \quad (13)$$

equiv of MeOH in 45% yield. Analogous reactions of compound **7** with two molar equiv of *p*-cresol or $HOCH_2C_6H_4$-4-*t*-Bu give $(Tolnacnac)_2Zr(OTol)_2$ (**20**, 67% yield) or $(Tolnacnac)_2Zr(OCH_2C_6H_4$-4-*t*-$Bu)_2$ (**21**, 92% yield), respectively.

In contrast to **16**, ^1H NMR spectra of **19** and **21** indicate chemically nonequivalent ligand methyl groups at room temperature. Line-shape analysis for methyl resonances of the ligand backbone in compounds **19** and **21** gives the following activation parameters for site exchange: (**19**) $\Delta H^{\ddagger} = 13(1)$ kcal/mol, $\Delta S^{\ddagger} = -9(4)$ eu; (**21**) $\Delta H^{\ddagger} = 13(1)$ kcal/mol, $\Delta S^{\ddagger} = -10(4)$ eu. The appearance of the methylene resonances in **21** is solvent dependent. In C_6D_6 or C_7D_8, the methylene resonance is a singlet at room temperature. VT NMR experiments show that the chemical shifts for the diastereotopic methylene protons are temperature dependent. Thus, the singlet at room-temperature results from an accidental degeneracy instead of site exchange. In $CDCl_3$, the diastereotopic protons resonate as two doublets ($|^2J_{HH}| = 13.5$ Hz). From line-shape analyses for $CDCl_3$ solutions, the activation parameters for methylene ($\Delta H^{\ddagger} = 14(1)$ kcal/mol and $\Delta S^{\ddagger} = -8(4)$ eu) and imine ($\Delta H^{\ddagger} = 13(1)$ kcal/mol and $\Delta S^{\ddagger} = -10(4)$ eu) exchange have been calculated.

Discussion

Synthetic Considerations. Aminolysis reactions are convenient methods for transferring ligands containing acidic protons. This approach is useful in the present case; however, certain thermodynamic and kinetic limitations prevent this route from providing a general synthetic entry. Deoxygenation by $Ti(NMe_2)_4$ has literature precedent in reactions involving 2,4-pentanedione and closely related ketiminate ligands.[42] Unlike chemistry reported for 2,4-pentanedione, we have not been able to isolate $(Tolnacac)_2Ti(NMe_2)_2$. For Zr, deoxygenation is not observed, and aminolysis is a suitable route to compound **1**. The failed attempts to prepare $(Tolnacac)Zr(NMe_2)_3$ contrast the chemistry of diketiminate complexes where five-coordinate, tris(dimethylamido) compounds can be prepared in high yield. Clearly, the intermediate $(Tolnacac)Zr(NMe_2)_3$ is more substitutionally labile than its diketiminate counterpart (**6**). This could be attributed to decreased steric interactions between the metal complex and the incoming ligand, a more highly acidic proton in TolnacacH relative to TolnacnacH, or a combination of both features.

While one or two Tolnacnac ligands can be introduced to a zirconium center, DipnacnacH failed to react with $Zr(NMe_2)_4$ under similar reaction conditions, presumably due to the steric demands of the ^{i}Pr substituents. However, DipnacnacH·HCl reacts with $Zr(NMe_2)_4$ to give $(Dipnacnac)ZrCl(NMe_2)_2$ (**7**) in moderate yield. Therefore the reaction of the protonated form of DipnacnacH represents an approach for circumventing kinetic limitations on amide transfer. The first event in this reaction sequence is likely proton transfer to generate intermediate $Zr(NMe_2)_3Cl$. Subsequent coordination of DipnacnacH should be more favorable due to a decrease in the steric bulk surrounding zirconium and increased electrophilicity at the metal center. Compound **7** may be a useful starting material for halide substitution and abstraction chemistry.

The recent report by Collins and co-workers has shown that the diketiminate amide complexes are useful synthons for preparing halide and cyclopentadienyl derivatives by protonolysis with $[NHMe_3][Cl]$ and $SiMe_3Cl$.[25] For zirconium complexes, conversion to chloride derivatives can also be achieved by refluxing the compounds in dry chloroform. Similar protolytic routes to alkoxide complexes from the amides and alcohols are effective for converting $(Tolnacnac)_2Zr(NMe_2)_2$ to $(Tolnacnac)_2Zr(OR)_2$; however, the reactions between $(Tolnacnac)Zr(NMe_2)_3$ and 3 equiv of MeOH give the alkoxides in extremely low yields. Significant quantities of free ligand in these reactions implicate competitive Tolnacnac alcoholysis as a major side reaction.

The most general method for preparing ketiminate and diketiminate starting materials is the reaction of the lithium salts with corresponding metal halides. Problems that arise from deoxygenation by $Ti(NMe_2)_4$ are avoided, and complexes with the formula *cis*-L_2TiCl_2 (**9** and **11**) can be prepared in good yield. Reactions of diketiminate lithium salts with zirconium tetrachloride afford both mono- and bis(diketiminate) complexes. Compounds with the formulas $LMCl_3$ can be prepared for titanium (L = Tolnacnac) and zirconium (L = Dipnacnac) via simple salt elimination reactions. For Zr, the bis(diketiminate) derivative **16** can be prepared in good yield. The only problem associated with the lithium salt route arises when competitive ligand substitution rates yield mixtures of mono- and disubstituted diketiminate complexes in the attempted preparation of compound **15** from $ZrCl_4$.

Structural Features. In the six-coordinate dichloride bis(ketiminate) and bis(diketiminate) compounds, the chloride stereochemistry is cis. For the ketiminate complexes, stereoisomers with mutually cis oxygen (**A**) or nitrogen (**B**) atoms are observed (Chart 2). Due to the presence of the aryl group,

Chart 2

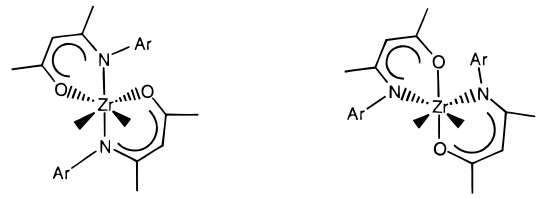

steric interactions are greater for isomer **B** relative to isomer **A**. The observation that the cis-oxygen stereoisomer is favored with increased steric bulk of the imine aryl group is consistent with this notion. There is no significant variation in Ti−N, Ti−O, and Ti−Cl distances in compounds **9** and **11**. Thus, the trans influence of the ligand on the Ti−Cl bond appears to be insensitive to the orientation of the N and O donors.[43,44] There are significant differences in bond distances of the ligand backbones for ketiminate and diketiminate structures. The two C−C distances within the conjugated ketiminate framework differ significantly. The differences between the long and short bonds in compounds **1** and **9**−**11** range from 0.07 to 0.08 Å

(42) Weingarten, H.; Miles, M. G. *J. Org. Chem.* **1968**, *33*, 1506−1508.

(43) Cozzi, P. G.; Floriani, C.; Chiesi-Villa, A.; Rizzoli, C. *Inorg. Chem.* **1995**, *34*, 2921−2930.

(44) Cozzi, P. G.; Solari, E.; Floriani, C.; Chiesi-Villa, A.; Rizzoli, C. *Chem. Ber.* **1996**, *129*, 1361−1368.

reflecting a major contribution from resonance structure **C** in Chart 3. The metrical data for the backbone are insensitive to

Chart 3

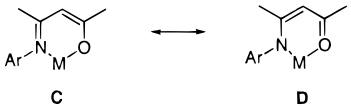

trans ligands and ketiminate stereochemistry. The variations in C−C and C−N distances in the diketiminate ligands in compounds **5**, **6**, **8**, **13**, **16**, and **17** are less pronounced with only one structure (**5**) having a difference beyond 3σ. This is consistent with greater delocalization that is expected from the increased symmetry of the conjugated π-system.

Compounds **10** and **16** also provide a comparison between inner coordination spheres of Tolnacac and Tolnacnac complexes. The Zr−N distance in compound **10** is substantially longer than the Zr−N distances for the cis N atoms and shorter than the Zr−N distances for the trans N atoms in compound **16**. Despite the shorter Zr−N distances for the cis N atoms in compound **16**, the Zr−Cl distances in compounds **10** and **16** are essentially identical.

An analogue to ketimine adduct, **4**, has been reported by Kogan et al.[45] In lieu of structural characterization, the authors proposed trans stereochemistry and suggested resonance form **E** in Chart 4 as the major contributor. This assignment was based

Chart 4

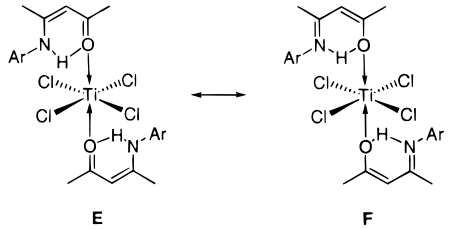

primarily on IR data. In particular, an absorption was observed at 3170 cm^{-1}, which was assigned to an N−H vibration participating in a hydrogen bond. Resonance structure **F** was discounted since a characteristic iminium band at 2250 cm^{-1} was not detected. In the context of this previously proposed structure, the structural features of compound **4** merit discussion. The C−O distance (average = 1.301(8) Å) in compound **4** is longer than those observed in $TiCl_4$−carbonyl adducts (1.18(3)−1.244(16)),[44,46−48] and the C(2)−C(3) (1.362(7) Å) and C(3)−C(4) (1.418(7) Å) distances favor an enolimine tautomer for the ketimine ligand (**F**). This situation is the reverse of that found for free ketimines, which are localized toward a ketoenamine limiting resonance form (**E**) where C(2)−C(3) is longer than C(3)−C(4).[49] The localized bonding in compound **4** parallels that found in the η^2-ketiminate compounds. Apparently, the tautomeric shift results from coordination of the oxygen to a group that is sufficiently electron deficient to shift the electron density relative to that in the free ketimine ligand.

The five-coordinate complexes in the present work adopt both trigonal bipyramidal and square pyramidal structures. Trigonal bipyramidal structures are found for compounds **5** and **6**. For compounds **8** and **17**, square pyramidal geometry is observed at Zr. For compound **8**, a dimethylamide group occupies the apical position in the square pyramid. This is consistent with the observation that the strongest donor ligands prefer coordination at this site. Dissection of the factors that contribute to a shift in geometry from trigonal bipyramidal for the amide complexes **5** and **6** to square pyramidal for compounds **8** and **17** is nontrivial. A recent theoretical treatment found that a square pyramidal structure is favored relative to a trigonal bipyramidal structure for d^0 complexes with pure σ-donating ligands.[50] The C_{4v} gas-phase structure of $TaMe_5$ supports this conclusion.[51] From a steric viewpoint, the trigonal bipyramidal structure minimizes interligand repulsions and will be favored when steric factors dominate. However, π-interactions in compounds **5**, **6**, **8**, and **17** are likely significant and may muddle steric and electronic distinctions, and the aryl substituents of the diketiminate ligands in compounds **5** and **6** differ from those in compounds **8** and **17**. We have observed that square pyramidal structures are also preferred for related alkyl compounds where π-interactions are minimized.[31]

In the trichloride compound, **13**, the Tolnacnac ligand functions as a six-electron donor. The deviation form planarity for the ligand backbone implicates contributions from an allyldiimine resonance form that was first suggested by Lappert for a closely related zirconium compound.[52] Contributions from resonance structure **G** (Chart 5) probably account for distortion

Chart 5

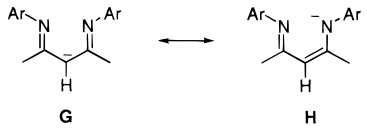

of C(3). The Ti−C(3) distance in **13** (2.535(4) Å) is significantly longer than Ti−C distances to the central carbons in pentadienyl structures (2.27−2.32 Å)[53,54] and even longer than the Ti−C distance in the β-agostic compound [$Ti(Me_2PCH_2CH_2PMe_2)EtCl_3$] (2.516(10) Å).[55] The metrical parameters imply that the M−C interactions in η^5-diketiminates are weaker than those in pentadienyl complexes. The observed $\eta^5 \rightarrow \eta^2$ shift of the diketiminate ligand when Lewis bases are added to compound **15** (vide infra) supports this notion since pentadienyl ligands are generally inert toward ligand substitution.[56] The deshielding of the methine proton appears to be diagnostic for η^5-coordination.[57] Although we have not determined the structure for the zirconium analogue, the pronounced deshielding of the methine proton in compound **15** parallels that observed in compound **13**. When thf is added to **15**, compound **14** is

(45) Kogan, V. A.; Sokolov, V. P.; Osipov, O. A. *J. Gen. Chem. USSR (Engl. Transl.)* **1970**, *40*, 812−817.
(46) Poll, T.; Metter, J. O.; Helmchen, G. *Angew. Chem., Int. Ed. Engl.* **1985**, *24*, 112−114.
(47) Kakkonen, H. J.; Pursiainen, J.; Pakkanen, T. A.; Ahlgrén, M.; Iiskola, E. *J. Organomet. Chem.* **1993**, *453*, 175−184.
(48) Sobota, P.; Szafert, S.; Lis, T. *J. Organomet. Chem.* **1993**, *443*, 85−91.
(49) Dasilva, Mavr; Dasilva, Mdmcr; Paiva, J. P. A.; Nogueira, Imcs; Damas, A. M.; Barkley, J. V.; Harding, M. M.; Akello, M. J.; Pilcher, G. *J. Chem. Soc., Perkin Trans. 2* **1993**, 1765−1769.
(50) Landis, C. R.; Kirman, T. K.; Root, D. M.; Cleveland, T. *J. Am. Chem. Soc.* **1998**, *120*, 1842−1854.
(51) Pulham, C.; Haaland, A.; Hammel, A.; Rypdal, K.; Verne, H. P.; Volden, H. V. *Angew. Chem., Int. Ed. Engl.* **1992**, *31*, 1464−1467.
(52) Hitchcock, P. B.; Lappert, M. F.; Liu, D.-S. *J. Chem. Soc., Chem. Commun.* **1994**, 2637−2638.
(53) Gedridge, R. W.; Arif, A. M.; Ernst, R. D. *J. Organomet. Chem.* **1995**, *501*, 95−100.
(54) Ernst, R. D.; Freeman, J. W.; Stahl, L.; Wilson, D. R.; Arif, A. M.; Nuber, B.; Ziegler, M. L. *J. Am. Chem. Soc.* **1995**, *117*, 5075−5081.
(55) Dawoodi, Z.; Green, M. L. H.; Mtetwa, V. S. B.; Prout, K. *J. Chem. Soc., Chem. Commun.* **1982**, 802−803.
(56) Ernst, R. D. *Chem. Rev.* **1988**, *88*, 1255−1291.
(57) Kuhn, N.; Kuhn, A.; Boese, R.; Augart, N. *J. Chem. Soc., Chem. Commun.* **1989**, 975−976.

Table 10. Results of Eyring Plot of Rates Derived from Full Line-Shape Analysis

	$\Delta H^{\ddagger}$ (kcal/mol)	$\Delta S^{\ddagger}$ (eu)	T_c (°C)[c]	solvent
(Tolnacnac)$_2$ZrCl$_2$ (**16**)	8.5(3)	−13.4(4)	−31	C_7D_8
(Tolnacnac)$_2$Zr(OMe)$_2$ (**19**)	12.7(6)	−9.3(5)	46	C_7D_8
(Tolnacnac)$_2$Zr(OBn′)$_2$ (**21**)[a]	13.0(4)	−10.2(3)	65	$CDCl_3$
(Tolnacnac)$_2$Zr(OBn′)$_2$ (**21**)[b]	13.6(5)	−8.2(4)	41	$CDCl_3$
(Tolnacnac)$_2$Zr(OBn′)$_2$ (**21**)[a]	12.2 ± 1	−12.5(4)	63	C_7D_8

[a] Tolnacnac ligand methyl site exchange OBn′ = $OCH_2C_6H_4$-4-*t*-Bu. [b] Methylene in OBn′ site exchange. [c] T_c determined in a 300 MHz ^{1}H NMR spectrometer.

generated, and the methine proton is shifted to higher field. These features and Lappert's early observation of similar η^5-binding strongly support η^5-coordination in **15**.[1,52] The structure for compound **17** shows that substitution at the aryl *ortho* positions can prevent η^5-coordination. It is not obvious whether steric or electronic effects of the Dipnacnac ligand dictate η^2-coordination in compound **17**. The zirconium center in this compound **17** is kinetically accessible to external nucleophiles as formation of the thf adduct, (Dipnacnac)ZrCl$_3$(thf), indicates.

Solution Behavior. Several of the compounds in this paper exhibit fluxional behavior. As expected, site exchange between chemically nonequivalent sites in the five-coordinate complexes **5**, **6**, and **8** has been observed. For compound **5** and **6**, this exchange is rapid; however, in compound **8** broad resonances are observed at ambient temperature for the dimethylamide methyl and Dipnacnac isopropyl resonances. Although these resonances sharpen at elevated temperatures, low-temperature ^{1}H NMR spectra for compound **8** are complex and cannot be interpreted simply in terms of the solid-state structure.

For compound **5**, a slow-exchange limit is reached and NMR data are consistent with the solid-state structure, which indicates η^2-Tolnacnac coordination at axial and equatorial positions. The three sets of amide methyl resonances can be explained by hindered rotation about the Ti−N bonds for the equatorial dimethylamido ligands, which places two methyl groups syn and two methyl groups anti to the apical dimethylamido ligand. Due to pseudomirror symmetry at the apical position, a single resonance for the apical amide methyl groups is expected even if rotation about the Ti−N bond is slow. The slow-exchange limit has not been reached for compound **6**. Given the larger radius for zirconium (Table 5), steric barriers to pseudorotation around Zr−N bonds should be lower than for compound **6**.

Collins recently reported chemical exchange between cis and trans nitrogen sites in *cis*-(Phnacnac)$_2$ZrCl$_2$. A Bailar-twist mechanism was proposed to account for this exchange (Scheme 1). Similar exchange is observed for compounds **16**, **19**, and

Scheme 1

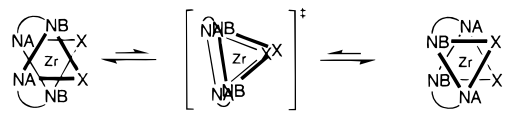

21. The activation parameters in Table 10 exhibit negative values for $\Delta S^{\ddagger}$, which indicate an ordered transition state as expected for a Bailar-twist mechanism. The activation parameters ($\Delta H^{\ddagger}$ = 8.5(3) kcal/mol; $\Delta S^{\ddagger}$ = −13.4(4) eu) for compound **16** are virtually identical to those reported for *cis*-(Phnacnac)$_2$ZrCl$_2$ ($\Delta H^{\ddagger}$ = 9(1) kcal/mol; $\Delta S^{\ddagger}$ = −10(1) eu).[25] For compounds **19** and **21**, ^{1}H NMR spectra at ambient temperature indicate slow exchange on the NMR time scale, and $\Delta H^{\ddagger}$ (**19**, 12.7(6) kcal/mol, C_7D_8; **21**, 13.0(4) kcal/mol, $CDCl_3$) is significantly larger than for the dichloride analogue. In compound **21**, reliable activation parameters for Tolnacnac methyl exchange can be determined for C_7D_8 solutions; however, the exchange between diastereotopic methylene resonances is complicated by temperature-dependent chemical shifts, which result in an accidental degeneracy below the coalescence temperature. In $CDCl_3$, the methylene chemical shifts remain constant and activation parameters for both sites can be compared. Activation parameters for methyl ($\Delta H^{\ddagger}$ = 13.0(4) kcal/mol; $\Delta S^{\ddagger}$ = −10.2(3) eu) and methylene ($\Delta H^{\ddagger}$ = 13.6(5) kcal/mol; $\Delta S^{\ddagger}$ = −8.2(4) eu) exchange are nearly identical. The errors for the activation parameters may be underestimated since line shape analysis is limited to a relatively narrow temperature range. Although temperature dependence of $\Delta H^{\ddagger}$ can lead to inaccuracies when rates are measured over a broad temperature ranges, deviations from Arrhenius behavior result in nonlinear plots of ln(k/T) vs 1/T.[58] Because the data from Eyring plots for steriosomerism of compounds are linear, it is unlikely that the temperature dependence of $\Delta H^{\ddagger}$ is significant over the temperature regimes examined. The parameters derived from the line shapes of the methyl resonances of compound **21** in $CDCl_3$ and C_7D_8 are comparable, indicating a minimal solvent effect on the isomerization.[58] Thus, agreement of the activation parameters is consistent with one mechanism that exchanges both methylene and Tolnacnac sites. The Bailar-twist mechanism that accounts for Tolnacnac site exchange in Scheme 1 also interconverts Λ and Δ enantiomers. Hence, the process that exchanges the Tolnacnac methyl sites will necessarily exchange the diastereotopic methylene protons. The inversion of configuration through Bailar-twist mechanism described here contrasts that for related 8-quinolinolato compounds, which interconvert via dissociative mechanisms.[59]

The difference in $\Delta H^{\ddagger}$ between compound **16** and compounds **19** and **21**, and the observation that (Tolnacnac)$_2$Zr(NMe$_2$)$_2$ (**7**) is stereochemically rigid on the NMR time scale, could be attributed to steric effects. The shorter Zr−O bond length relative to Zr−Cl and the presence of alkoxide alkyl substituents will increase steric repulsion in the transition state for bis(alkoxide) complexes relative to compound **16** in the Bailar-twist mechanism. Thus, the increase in $\Delta H^{\ddagger}$ for the bis(alkoxide) compounds in Table 10 is consistent with the proposed mechanism for isomerization. For compound **7**, steric interactions are more severe since the dimethylamido ligands have two alkyl substituents compared to one for the alkoxide ligands. However, electronic contributions could also dominate since increased π-donation has been predicted to stabilize pseudooctahedral geometries relative to trigonal prismatic structures. Density functional calculation showed that d^0 transition metal complexes (ML$_6$) prefer pseudo-trigonal prismatic, instead of octahedral, geometries when L is a σ-only, or weak π-donating, ligand.[60] When the ligands are strong π-donors, an octahedral geometry is preferred. This is supported by the behavior of W(pinacolate)$_3$. For this complex, exchange of chemically inequivalent methyl sites is not observed on the NMR time scale, which establishes a lower limit of 15 kcal mol^{-1} at 110 °C for the energy difference between the D_3 ground state and the D_{3h} transition state.[61] Thus, the barrier increase in the order of Cl < OR < NR$_2$ could solely be due to, or reinforced by, electronic

(58) Zavitsas, A. A. *J. Am. Chem. Soc.* **1997**, *119*, 6578−6586.
(59) Bei, X.; Swenson, D. C.; Jordan, R. F. *Organometallics* **1997**, *16*, 3282−3302.
(60) Kaupp, M. *Chem. Eur. J.* **1998**, *4*, 1678−1686.
(61) Chisholm, M. H.; Parkin, I. P.; Streib, W. E.; Eisenstein, O. *Inorg. Chem.* **1994**, *33*, 812−815.

destabilization of a trigonal prismatic excited state relative to the pseudooctahedral ground state.

Conclusions

Ketiminate and diketiminate complexes can be conveniently prepared by several synthetic routes. As previously demonstrated by Collins, aminolysis reactions of $Ti(NMe_2)_4$ and $Zr(NMe_2)_4$ afford certain diketiminate compounds in good yield. These approaches are limited for preparing ketiminate titanium compounds, where deoxygenative amide transfer can occur, and for synthesizing compounds from sterically encumbered diketimines.

Protonated and deprotonated forms of the neutral ligands can be used to circumvent these problems. In acid−base transfer reactions, the reaction rates for the protonated diketimine ligands are greatly enhanced relative to the neutral ligand. Presumably, this is due to a rapid proton transfer to the leaving group on the metal and generation of a kinetically viable intermediate that can react with the neutral ligand in a second base-elimination step. Anionic sources of ketiminate and diketiminate ligands are the most versatile synthetic reagents in this family. Several useful starting materials can be prepared directly from metal halides, and problems that arise from ligand deoxygenation can be thus prevented.

The aryl substituents on the diketiminate ligand can influence the diketiminate binding mode. For the Tolnacnac ligand, η^5-binding is confirmed for (Tolnacnac)$TiCl_3$ and is likely the coordination mode in (Tolnacnac)$ZrCl_3$. For Dipnacnac, the ligand derived from 2,6-diisopropylaniline, η^2-binding is found for (Dipnacnac)$ZrCl_3$. For (Dipnacnac)$ZrCl_3$, and other five-cooridinate diketiminate complexes, square pyramidal geometry is preferred, and trigonal bipyramidal structures are observed only for the tris(amido) derivatives (Tolnacnac)M-$(NMe_2)_3$ (M = Ti, **5**; M = Zr, **6**). The five-coordinate compounds are all fluxional in solution, and low-temperature NMR spectra consistent with the solid-state structures are only observed for (Tolnacnac)$Ti(NMe_2)_3$.

The stereochemical rigidity of the (Tolnacnac)$_2ZrX_2$ derivatives where X is a uninegative ligand is sensitive to variations in X. The Λ and Δ enantiomers interconvert by a Bailar-twist mechanism, and the relative ordering for rates of exchange at a common temperature follows the order Cl > OR > NR_2. The trend in rates parallels the anticipated increase in the steric repulsion in the Bailar-twist transition state, Cl < OR < NR_2, and is consistent with the increase in $\Delta H^{\ddagger}$ for alkoxide derivatives relative to the dichloride complex, **16**. The six-coordinate complexes whose isomerizations are sufficiently slow on the NMR time scale offer possibilities for potential catalytic applications. We plan to explore these possibilities and assess the utility of diketiminate ligands for stabilizing unusual coordination geometry in transition metal systems.

Acknowledgment. We appreciate support from the National Science Foundation (Grant CHE-9817230). We are also grateful for financial support through an All University Research Initiation Grant and the Center for the Fundamental Material Research at MSU. D.H.M. thanks the Research Council of Kent State University for a research grant and B.Q. is grateful for a Carl H. Brubaker Endowed Fellowship. The single-crystal X-ray equipment at MSU was supported by the National Science Foundation (Grant CHE-9634638), and the NMR equipment was provided by the National Science Foundation (Grant CHE-8800770) and the National Institutes of Health (Grant 1-S10-RR04750-01).

Supporting Information Available: X-ray crystallographic files in CIF format for the structure determinations of **1**, **4**−**6**, **8**−**11**, **13**, **16**, and **17**. This material is available free of charge via the Internet at http://pubs.acs.org.

IC981364J